Available online at www.sciencedirect.com
SCIENCE DIRECT®
Catalysis Today 86 (2003) 87–109
CATALYSIS TODAY
www.elsevier.com/locate/cattod

Encapsulation of transition metal sulfides in faujasite zeolite for hydroprocessing applications

E.J.M. Hensen [a], J.A.R. van Veen [a,b,*]

[a] *Schuit Institute of Catalysis, Eindhoven University of Technology, P.O. Box 513, 5600 MB Eindhoven, The Netherlands*
[b] *Shell Research and Technology Centre Amsterdam, Badhuisweg 3, 1031 CM Amsterdam, The Netherlands*

Received 9 April 2003; accepted 19 May 2003

Abstract

The dispersion of the sulfides of Co, Ni, Mo and W—and their combinations—in the micropores of acidic faujasite zeolite is a challenging task. While a close proximity of the hydrogenation function to the acidic cracking sites is thought to be beneficial for industrial hydrocracking applications, the genesis of well-defined metal sulfides in a tunable environment allows to address two important fundamental issues: (i) the possible existence of an optimum cluster size of metal sulfides with respect to hydrodesulfurization activity and (ii) an extension of the well-known support effect in hydrotreating catalysis. This review will concentrate on the various preparation methods—ranging from the brute-force chemistry involved in dispersing anion precursors to the occlusion of well-defined organometallic complexes in the zeolite micropore space, characterization to determine the successful genesis of suitable models and activity tests.

Successful dispersion of these sulfides in the micropores of faujasite is only possible by careful preparative methods, either using well-dried cation-exchanged precursors or organometallic complexes. A synergistic effect of acidic protons on the metal sulfides is noted. However, the relatively low activities of ultra-dispersed Mo- or Co-sulfide particles compared to those of particles on more traditional supports force us to conclude that there must be an optimal size for metal sulfide clusters larger than those stabilized in the micropores. Although there are some indications that a sulfided CoMo cluster can be formed in the micropores using organometallic precursors, the synergistic effect between the two metals is quite small. From an application point of view, the detrimental effect of bases such as water or nitrogen compounds to the final dispersion of the metal sulfides is problematic. Nevertheless, model studies indicate that a close proximity of acidic and hydrogenation components decreases coking deactivation.

Keywords: Hydrotreating; Hydrocracking; Metal sulfides; Acidic zeolite; Dispersion; Support

1. Introduction

Hydrotreating is one of the key processes in a modern oil refinery for the production of clean motor fuels. It refers to such processes as hydrodesulfurization (HDS), hydrodenitrogenation (HDN) and hydrodearomatization (HDA). The main driver for the continuing need for improved hydrotreating catalysts is increasing environmental awareness. More stringent legislative rules mainly limiting the sulfur and aromatics content in transportation fuels are prescribed in the USA and Europe. It is anticipated that zero-sulfur levels will be enforced on a 5–10 years time span. This will necessitate further optimization of current processes (better catalysts and

* Corresponding author.
E-mail address: rob.vanveen@shell.com (J.A.R. van Veen).

0920-5861/$ – see front matter © 2003 Elsevier B.V. All rights reserved.
doi:10.1016/S0920-5861(03)00406-1

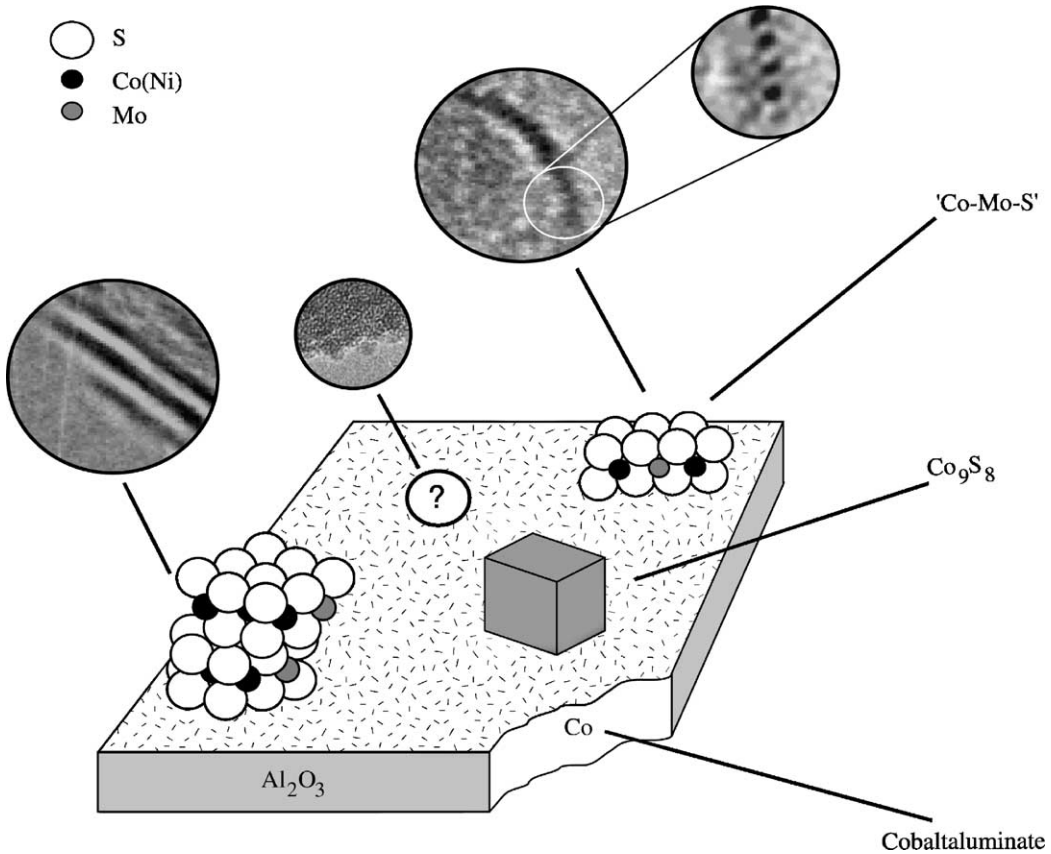

Fig. 1. Schematic representation of the various catalytic species present in a commercial γ-alumina-supported CoMo-sulfide catalyst. The transmission electron micrographs display the layered nature of the MoS_2 phase. Next to these slab-like structures with sizes in the range of 2–5 nm—possibly promoted by Ni or Co, bulky cobalt (nickel) sulfide species with a low activity and inactive cobalt (nickel) strongly interacting with the support are present. An additional phase is presented by relatively small oxysulfide particles after mild sulfidation [2].

process arrangements) and most likely require the application of alternative processes for sulfur removal [1]. Modern hydrotreating catalysts mainly consist of Co/Mo, Ni/Mo or occasionally Ni/W mixed sulfides supported on a high-surface-area γ-alumina support (Fig. 1). Deep hydrodesulfurization of gas oil may also be achieved by employing noble metal catalysts. A number of reviews on the state-of-art in this field are available [3–7].

Whereas these medium-pressure hydrotreating processes do not result in a decrease of the molecular weight of the product, hydrocracking of higher-boiling fractions, typically carried out above 100 bar hydrogen pressure, is employed to arrive at economically more profitable products such as gas oil and kerosene. The latter process is still gaining in importance, mainly because of the excellent product properties including very low sulfur contents and very good combustion properties. Hydrocracking typically requires bifunctional catalysts: they contain both acidic cracking and hydrogenation functions [8–10]. The acidity is normally provided by (stabilized) faujasite zeolites, although amorphous silica–alumina is also used for mild hydrocracking. Hydrogenation is provided by Ni/W mixed sulfides, Ni/Mo mixed sulfides in the case nitrogen removal is important and Pd when sulfur concentrations are low as encountered in some two-stage configurations [10].

The genesis of small metal sulfide particles encaged in the intrazeolite pores offers several interesting

perspectives. Foremost, the well-defined three-dimensional pore network endows these materials with the possibility to stabilize very small, uniformly shaped metal sulfide particles in a tuneable environment. As such, it forms an extension of the support effect in hydrotreating catalysis. For instance, the choice of support pronouncedly influences the catalytic activity of MoS_2- or WS_2-based catalysts [11,12], be it through the extent of the metal–support interaction, the resulting dispersion and morphology or the support acidity [13]. Generally, dispersing metal sulfides on high-surface-area supports results in particles of widely varying size and morphology [4]. One of the possible strategies for improving hydrotreating catalysts may be to significantly improve the dispersion of supported transition metal sulfides. The question, however, is whether there is an optimum in activity as a function of the particle size and whether ultra-small particles stabilized in a zeolite matrix have any special catalytic properties.

A more practical motive for the extensive research in the field of zeolite-supported metal sulfides relates to industrial hydrocracking catalyst. Generally, the (de)hydrogenation component and the acidic cracking function are spatially separated by several microns. However, a close proximity of these two functions may be important for two reasons. In the first place, naphthenes present in industrial feeds are precursors to coke via bimolecular hydrogen transfer reactions with olefins or other aromatics. The presence of a hydrogenation function close to the acid sites where these aromatic coke precursors tend to adsorb may decrease coking deactivation. Secondly, it may be important to obtain 'ideal hydrocracking' [10], since large diffusion distances may disturb the equilibrium composition of olefins at the acidic sites. Encapsulation of the hydrogenation function in the zeolite pores close to the Brønsted hydroxyl groups may thus answer the question if there is any advantage of a close proximity of these two.

This contribution will summarize the various methods to prepare zeolite-encaged metal sulfide clusters. We will evaluate if such methods result in the desired well-defined metal sulfide clusters, and finally by discussing the activity of model catalyst systems—focussing on the effects of dispersion, the support nature, catalyst stability and proximity of different functions—we hope to indicate if and how all this knowledge is of value to catalyst development. We will limit the scope of this review mainly to cobalt, nickel and molybdenum in zeolite Y, however touching upon other metals and porous support materials to provide a complete picture.

1.1. The zeolite matrix: faujasite

The high thermal and chemical stability of faujasite zeolite combined with its relatively large apertures allowing entrance to the large oil feedstock molecules renders this material the most applied support material for hydrocracking catalysts. It provides a strong cracking functionality in the form of the primary Brønsted acid sites. Zeolite Y with its well-defined pore topology (Fig. 2) and tunable ion-exchange properties presents an excellent model for fundamental studies.

The zeolite framework of the zeolites X and Y isomorphs is made up by connecting silicon- or aluminum-containing oxygen tetrahedra and results in hexagonal prisms, sodalite cages and supercages with maximum entrances of 2.6, 2.6, 7.4 Å and diameters of 2.6, 6.6 and 11.8 Å, respectively (Fig. 2). The negative charge introduced by the substitution of tetravalent silicon by trivalent aluminum is typically compensated by the presence of cations, although an important exception is provided by compensation with protons rendering the zeolite strongly acidic. The cations are localized at discrete positions, in the hexagonal prisms (site I), in the sodalite cages (sites I′ and II′) and in the supercages (sites II, III and III′). This depends on the type of cation, the loading and hydration state. In contrast, the location of metal sulfide particles is restricted to the supercages in most cases.

Although the development of industrial hydrocracking catalysts is largely limited to faujasite, its versatility is underlined by the vast number of modifications, including calcination, steaming, ion-exchange and leaching, allowing catalyst manufacturers to tailor this material for particular applications. Generally, there is a preference to use ultrastabilized Y (USY) or very ultrastabilized Y (VUSY) type zeolite materials due to their higher thermal and chemical stability. Additionally, the creation of mesopores reduces mass-transfer limitations. However, the non-uniformity of the pores makes those zeolites less suitable for fundamental

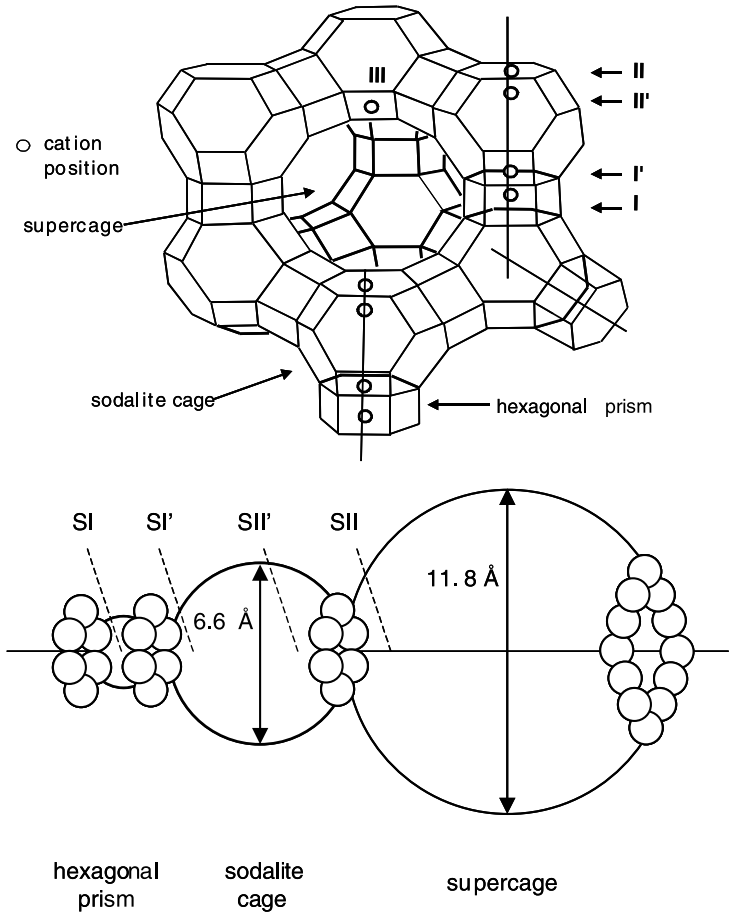

Fig. 2. The structure of faujasite or Y zeolite showing the sodalite cages, supercages and the hexagonal prism interconnections (top). A line drawing shows the size of the various pores in more detail including the location of the cation sites I and II (bottom).

studies. Other porous materials—including wide-pore zeolites like UTD-1, ordered mesoporous MCM- and SBA-type materials [14], silica–aluminas with regular pore diameters and pillared clays [15]—have also come in for their share of attention, but are outside the scope of this contribution.

1.2. Incorporation of Mo as anion

Impregnation of aqueous ammonium heptamolybdate (AHM) solutions, commonly applied for alumina supports, results in the external surface agglomeration of anionic Mo species in the case of zeolites. This is caused by the size of the oxoanionic or neutral complexes and the absence of anion-exchange properties of zeolites. At high pH, the equilibrium:

$$Mo_7O_{24}^{6-} + 4OH^- \leftrightarrows 7MoO_4^{2-} + 2H_2O \quad (1)$$

offers the advantage of the generation of MoO_4^{2-} species small enough to enter the micropores. A major drawback of this route is the dissolution of the zeolite lattice in the pH range where these species are stable. At neutral pH, $Mo_7O_{24}^{6-}$ species, that are too large to enter zeolite Y pores, are predominant. The presence of the oxidic precursor on the external surface of NaY zeolite was confirmed by TEM/EDX [16,17], nitrogen and Xe adsorption, ^{129}Xe NMR [16,18] and NO adsorption [19,20]. Although the majority of Mo species are present on the external surface, Welters et al. [16] observed that already after drying at least part of the

Mo phase is deposited in the zeolite pores. One possible cause is the migration into the pores of small MoO_4^{2-} ions either formed during impregnation (in low concentrations at neutral pH) [21] or during the drying step [16]. Alternatively, the drying step might lead to migration of MoO_3 from the external zeolite surface into the zeolite pores in the presence of residual water via the reaction:

$$MoO_3 + H_2O \leftrightarrows MoO_2(OH)_2 \quad (2)$$

as suggested by Fierro et al. [22]. During further calcination in ambient air additional Mo species enter the pores, which was explained by the presence of trace amounts of water in the calcination atmosphere. Based on reaction (2), the group of Fierro et al. [22–25] devised a method to redistribute MoO_3 species from the external surface into the zeolite pores in quasi-isothermal conditions maintaining a constant low water vapor pressure. The perturbation of the zeolite hydroxyl bands observed from IR and further DRS measurements [21] suggests the presence of molybdate species in close vicinity to the acid sites in line with more recent XANES investigations [26]. There are also some indications from ESR of the presence of some isolated Mo(V) ions in the sodalite cages or hexagonal prisms [22].

The incorporation of MoO_x species in the zeolite pores leads to a decrease of X-ray crystallinity [19,22] being more pronounced at higher Mo contents. Thoret et al. [27] also found strong lattice amorphization in their model study of the solid-state reaction between NaY and molybdenum trioxide. On the other hand, Cid et al. [28] observed that ion-exchange with Co^{2+} prior to Mo impregnation protects the zeolite against attack from the molybdate and results in a lower loss of crystallinity. A comparison between HY and NaY [19,28] indicates that the acidic support is more prone to the formation of amorphous zones to be explained by the lower stability of the HY lattice.

The information on the fate of the molybdenum oxide species in NaY upon sulfidation is rather scarce. Welters et al. [16] found that sulfidation results in an amount of intrazeolite Mo comparable to that present after calcination. Increasing metal content results in incomplete Mo sulfidation due to the presence of large MoO_3 particles on the external surface [16,18]. Although only a small part of the Mo-sulfide phase is dispersed in the zeolite micropore space, Welters et al. [16] attributed the high thiophene HDS activity of Mo/NaY to the occluded metal sulfide phase. EXAFS results of the group of Okamoto and Katsuyama [26] stressed the formation of tetrahedral Mo species which are more difficult to sulfide [29].

In the case of ultrastabilized Y-type zeolite, the presence of the secondary pore system presents a third location to Mo species. Several groups [17,25,30–39] have studied conventional impregnation of AHM on such materials. Most evident is the higher stability of the USY-type molecular sieves towards the molybdate species as evidenced by X-ray crystallinity measurements [17,32] and deduced from IR spectra of the hydroxyl region. Direct information on the location of the sulfide phases was extracted from combined TEM and EDX measurements of NiMo-sulfide on stabilized Y-type zeolites with low and high Si/Al ratios of 3 and 17 [35,36,39]. Whereas the large secondary pore volume of the latter samples allows accommodation of all the Ni and Mo ions in the oxidic precursor, only half of the Mo resides in the mesopores of the sample with $Si/Al = 3$, the remainder being present as MoO_3 particles on the external zeolite surface. Sulfidation converts the external crystallites into MoS_2 domains and results in a decrease of the amount of occluded metal species. Additional MoS_2 domains were observed mainly located in the mesopores as derived from their size and stacking degree. The slab size and stacking degree was found to be the largest for the most stabilized zeolite. From these results and those obtained from a TEM/EDX study of Mo impregnated on CaY [40], we conclude that the localization of Mo-sulfide species in the micropores is less favorable than in the mesopores. Sulfur analysis [31] and XPS intensity analysis of the metal-to-sulfur ratio [25,33] confirm the difficulty in fully transforming the external Mo phase into the sulfide. Essentially similar conclusions were reached in a recent study by Li et al. [17] showing the poor ability of microporous materials (NaY, mordenite and ZSM-5) to disperse Mo species in the smallest pores, although these authors have drawn the questionable conclusion that a small part of the sulfide phase in USY zeolite is located in the sodalite cages. The group of Payen and co-workers [41] studied the formation of the Anderson aluminomolybdate anion, $AlMo_6O_{24}H_6^{3-}$, in steamed zeolite Y. A combination of ^{27}Al MAS NMR, EXAFS and Raman spectroscopic measurements indicates that AHM impregnation

results in the formation of this anion in the pores via the interaction of AHM with extra-framework aluminum species. Although preserved during drying, this species decomposes into $Al_2(MoO_4)_3$ upon calcination. Unfortunately, the fate of the Anderson complex upon sulfidation is not known.

The impregnation of tungstate species on Y-type zeolites has been studied to a much lesser extent [40,42–44]. The study of Cid et al. [43] showed that impregnation at acidic pH leads to the inhomogeneous distribution of relatively small tungsten species in the USY zeolite, most probably in the mesopores and a small loss of crystallinity. These catalysts were much more active in thiophene HDS than a sample prepared by basic impregnation. This latter procedure results in the formation of W species on the exterior of the zeolite and removal of the larger part of its acidity.

In view of the above, it is fair to conclude that the incorporation of MoO_x or WO_x species in the pores of zeolite Y by conventional preparation routes is not successful. Although the dispersion of these oxides in the mesopores in stabilized faujasites has important industrial applications, it is less suitable for the preparation of well-defined model systems.

1.3. Incorporation of Mo as cation

An apparently more satisfactory method to load zeolite Y with Mo has been provided by Moorehead [45] and is based on ion-exchange with molybdenyl chloride MoO_2Cl_2. This compound cannot be used as such in aqueous solution since it readily hydrolyses according to

$$7MoO_2Cl_2 + 10H_2O \leftrightarrows Mo_7O_{24}{}^{6-} + 20H^+ + 14Cl^- \quad (3)$$

According to Minming and Howe [46] this problem can be overcome by applying a HCl/pyridine buffer at a pH of 4. The main drawback is the adsorption of quite an amount of pyridine by the molecular sieve, thereby limiting the Mo loading (Fig. 3a). In the case of VUSY, the use of pyridine to prevent acid decomposition of the zeolite is less pressing and we attempted to omit it altogether. To prevent the hydrolysis of molybdenyl chloride one needs fairly concentrated HCl solutions (∼2 N HCl) making ion-exchange difficult due to the high concentrations of protons. Simple pore-volume impregnation, however, is possible and results in a well-dispersed MoO_x phase. Raman spectra clearly show the adsorption of MoO_2Cl_2-type species in the impregnated precursor (Fig. 3b) which yields highly dispersed MoO_x species after calcination (Fig. 3c).

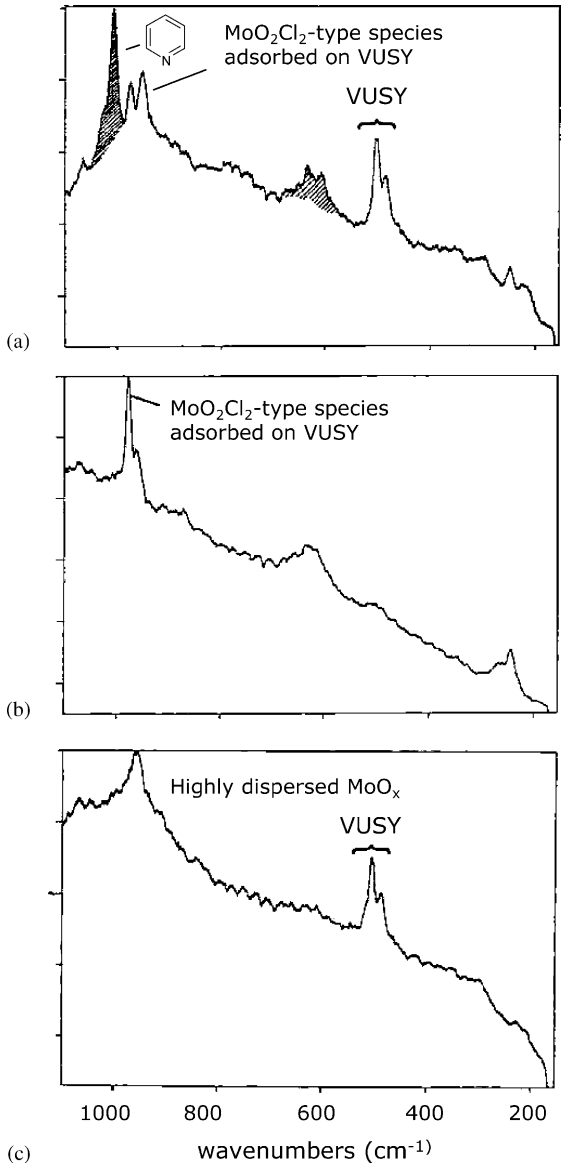

Fig. 3. Raman spectra of (a) ion-exchange of MoO_2Cl_2 from a pyridine/HCl buffer, clearly showing the strong adsorption of pyridine, (b) pore-volume impregnation of MoO_2Cl_2 with a 2 N HCl solution followed by drying at 120 °C and (c) sample b after calcination at 450 °C.

XRD reveals that no MoO_3 crystallites are present, leaving the crystallinity of the VUSY unaltered. A homogeneous metal distribution is indicated by XPS, in that the observed Mo-to-Al ratios are the same as the ones determined by elemental analysis. This is further underpinned by TEM/EDX and IR measurements of the hydroxyl stretching region showing a substantial reduction of the band intensities upon introduction of Mo. This derives from interaction of these groups with MoO_x moieties, implying at least a reasonable dispersion of the latter.

Solid-state exchange with $MoOCl_4$ [47], $MoCl_5$ [48] and MoO_3 under the action of CCl_4 [49] have also been described. Tatsumi and co-workers [50–55] have extensively studied the incorporation of the cationic molybdenum sulfide cluster $[Mo_3S_4(H_2O)_9]^{4+}$ by aqueous ion-exchange in several zeolites (NaY, HUSY, NaMOR and KL). The structure of this cluster with an incomplete cubane structure was shown to be maintained by UV-Vis and X-ray absorption spectroscopy after ion-exchange. Thermal treatment at 573 K converts the cluster into MoS_2-like species for Mo_3S_4/MOR and Mo_3S_4/NaY. The authors claim that the initially high dispersion is maintained. Experiments at the Shell Research and Technology Centre indicate that this route has some problematic aspects [56]. The $[Mo_3S_4(H_2O)_9]^{4+}$ clusters are quite stable in an aqueous solution of pH = 1, but contacting such a solution with a (V)USY leads to leaching of Al from the framework due to this rather low pH. The leached Al ions then cause the pH of the solution to increase locally to about 4, resulting in the hydrolysis of the sulfide clusters and their precipitation on the external zeolite surface and also to some extent in the mesopores. The starting pH of the cluster solution can be increased by either evaporation of HCl or addition of ammonia, but in each case hydrolysis commences once the pH reaches the neighborhood of 3, making the solution unstable. In other words, this method is not so easy as it looks.

Nevertheless, the group of Tatsumi described the introduction of Ni^{2+} either by ion-exchange of the zeolite prior to introduction of $[Mo_3S_4(H_2O)_9]^{4+}$ or by ion-exchange with the bimetallic sulfide cluster $[Mo_3NiS_4Cl(H_2O)_9]^{3+}$ (vide infra). The catalytic data show promising activities in benzothiophene HDS and stress the importance of the presence of strong acid sites in their catalytic results, even in Mo_3S_4/NaY due to the exchange of Na^+ with protons in the ion-exchange step and due to the reduction of the cluster [55].

Finally, we mention the possibility to encapsulate heteropoly acid such as $H_3PMo_{12}O_{40}$ (PMo_{12}) or $H_3PW_{12}O_{40}$ (PWO_{12}) as 'ship-in-bottle' precursors to dispersed molybdenum or tungsten sulfide phases. Since these Keggin-type heteropoly oxometalates are too large to pass the windows of the supercages of Y-type zeolite, their preparation inside the supercages of faujasite has been attempted by several authors [57–59]. In both works the zeolite was dealuminated prior to encapsulation of the heteropoly acids. Mukai et al. [58] noted that the PMo_{12} cluster was not formed in the supercages of non-dealuminated HY, which was attributed to the decomposition of the complex due to basic Al sites. Our experience is that inclusion of a PWO_{12} complex is indeed possible in a VUSY, an essential point being the removal of extraframework aluminum ions which tend to interact with the tungstate. Especially, ^{31}P NMR provides a way to distinguish the complex in the mesopores (sharp resonance corresponding to the naked complex) and the complex encaged in the micropores (broad resonance [57]). However, this modification did not increase the hydrocracking performance.

1.4. Incorporation of Co^{2+} and Ni^{2+}

The aluminum-rich faujasite-type zeolites generally have excellent cation-exchange properties. The atomic dispersion of catalytically interesting transition metal ions in cation-exchanged precursors makes them suitable to generate dispersed metal sulfides upon sulfidation. A possible advantage is the close proximity of the resulting sulfide to the acidic function providing a tool to study the proximity effect. The acidity derives from the sulfidation procedure through

$$Me^{2+}\text{–}(Oz)_2 + H_2S \leftrightarrows MeS + 2Oz\text{–}H^+ \quad (4)$$

as an example for a divalent cation. The majority of catalytic studies in this field relate to the incorporation of Co^{2+} [28,40,60–67] and Ni^{2+} [18,40,61,68–79] in Y-type zeolites. Cobalt- and nickel-sulfide have attracted the most attention due to their importance in the formation of promoted MoS_2 or WS_2 phases, generally employed for hydrotreating [3–7]. Additionally, indications that in industrial CoMo-based

catalysts MoS_2 slabs merely act as a secondary support to maintain a highly dispersed state of Co-sulfide [80] have urged the groups of van der Kraan and de Beer to employ microporous zeolites to obtain insight into the activity of ultra-dispersed Co-sulfide particles in the absence of MoS_2 [61–67,69–71].

de Bont et al. [62,65] studied the evolution of cobalt species in NaY zeolite upon sulfidation by a combination of ^{57}Co Mössbauer emission spectroscopy (MES), extended X-ray absorption fine structure (EXAFS) spectroscopy and thiophene hydrodesulfurization activity measurements. In a systematic way the effect of preparation method (ion-exchange CoNaY and pore-volume impregnation Co/NaY), pretreatment (drying prior to sulfidation) and sulfidation temperature were evaluated. Fig. 4 shows the ^{57}Co MES spectra of CoNaY(wet), CoNaY(dried) and Co/NaY(dried). Careful analysis of these spectra shows that very small Co-sulfide species are already formed upon room temperature sulfidation. These species are presumably larger and/or better ordered in CoNaY(wet) and Co/NaY(wet, not shown here) as derived from the larger *quadrupole splitting* (QS). In the wet samples these small clusters are transformed via intermediate CoS_{1+x} into Co_9S_8-type clusters. These latter particles with an *isomer shift* (IS) of 0.25 mm s^{-1} and a QS of 0.21 mm s^{-1} are comparable to bulky Co-sulfide particles formed in alumina-supported Co upon sulfidation at 673 K [81]. Such particles are most likely present at the external zeolite surface.

Conversely, the MES results point to a stronger bonding of the Co atoms to the zeolite lattice already in the dried precursor. This stems from the migration of hydrated Co^{2+} ions from the supercages [82] to cation positions [82,83]. Sulfidation results in spectra with one Co-sulfide doublet (IS $\approx$ 0.2 mm s^{-1}) and one asymmetric doublet with a wide distribution of IS and QS values indicative for the presence of a wide range of particles with varying size and/or ordering. Although the QS decreases for both doublets, no Co_9S_8-type species are formed upon sulfidation at 673 K. These results are condensed in Fig. 5 stressing the formation of smaller, disordered particles in the dried precursors and large, ordered particles in the non-dried case.

TEM micrographs provide further evidence that the Co_9S_8-type particles formed in sulfided CoNaY(wet) end up at the external zeolite surface, whereas the larger part of Co is highly dispersed in the zeolite micropore space in CoNaY(dry). Additional Co K-edge EXAFS measurements [65] unequivocally show the presence of a Co_9S_8-type phase in CoNaY(wet) with corresponding Co–Co distances which are absent in the sulfided catalyst derived from the dry precursor. The most important conclusion from this work is the beneficial effect of removal of intrazeolite water from the hydration shells of the cations on the final dispersion of the metal sulfide. A molecular explanation stresses the stronger cation–zeolite interaction in the dried precursor which hinders agglomeration of the Co-sulfide particles during the sulfidation procedure.

Fig. 6 shows that the thiophene HDS activities of CoNaY(dry) for various sulfidation temperatures are superior to those of CoNaY(wet). The lower activity of CoNaY (dry) upon sulfidation at 673 K was initially attributed to a small loss of dispersion of the intrazeolite Co-sulfide phase. However, the reason is more complex: Vissenberg et al. [64,66] observed that sulfided CoNaY(dry) is unstable at high temperatures and decomposes in cations and hydrogen sulfide leading to a dramatic loss in activity. This was serendipitously discovered by the observation that exposure to inert atmosphere of sulfided CoNaY(dry) results in a bluish color instead of the normally observed black color of the cobalt sulfide phase. This phenomenon is observed upon exposure to He, N_2 or Ar at 673 K after sulfidation. Similar changes take place in the sulfidation mixture at 773 K or alternatively after prolonged sulfidation at 673 K (at least 8 h). This transformation is accompanied by a loss of sulfur in the form of hydrogen sulfide as determined from metal-to-sulfur ratios [64]. Next to these physicochemical changes it was noted that such treatments result in a dramatic loss of HDS activity (Fig. 6). Hence, it was concluded that these species are inactive and possibly not accessible to thiophene. The Mössbauer parameters of these Co species could not be related to those of any known Co compound [63,64,66]. Further evidence for their relocation to inaccessible positions was provided by a strong decrease in oxygen chemisorption, a strong decrease in the NO IR bands assigned to Co-sulfide species, ^{129}Xe NMR measurements and their resistance to resulfidation. ESR measurements excluded the presence of S_3^- radicals in the sodalite cages as a possible explanation for the blue color. These data

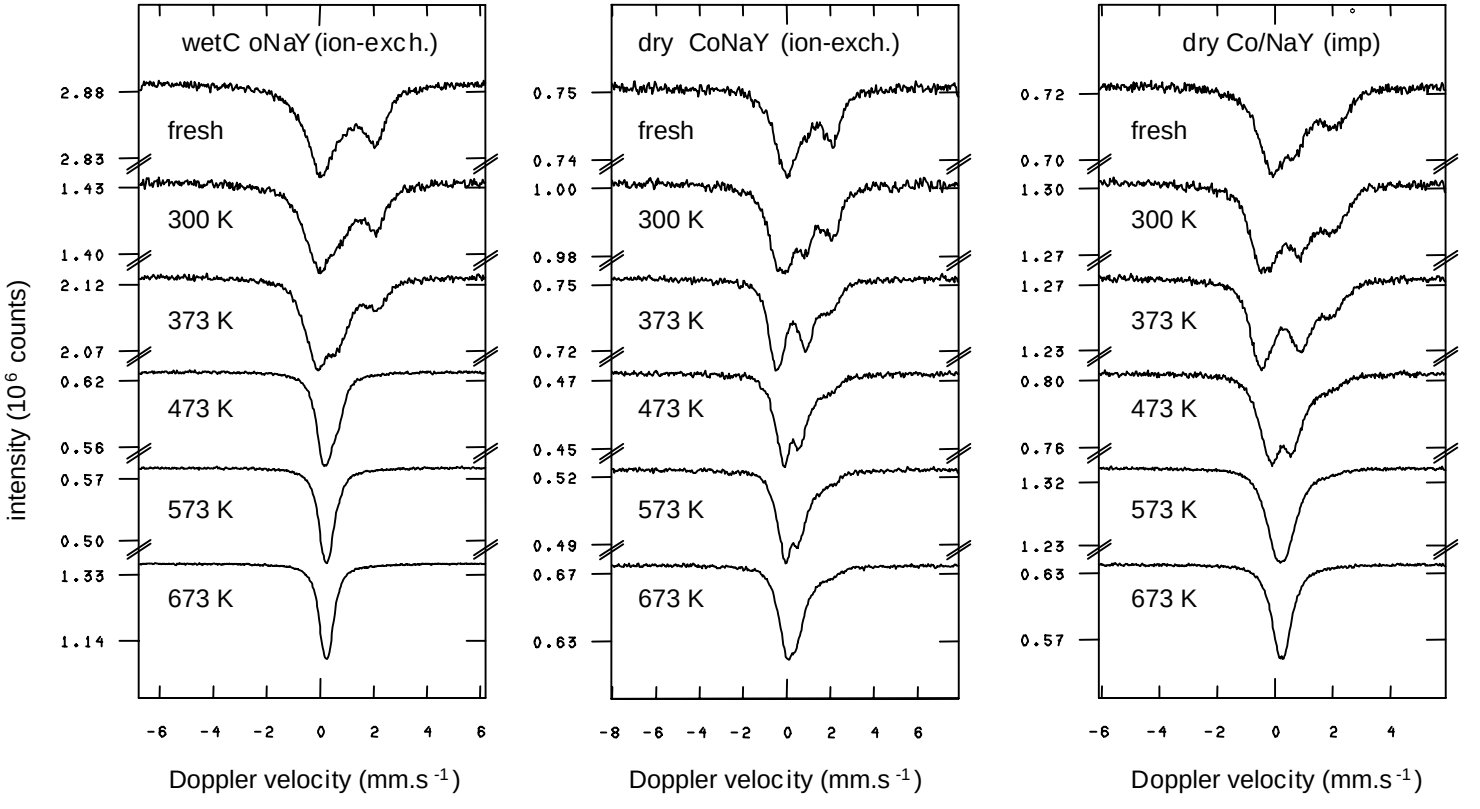

Fig. 4. ^{57}Co Mössbauer emission spectra of CoNaY(wet), CoNaY(dry) and Co/NaY(dry) in the fresh state and stepwise sulfided. In all cases, one observes the disappearance of the high-spin 2+ contribution and the appearance of a Co-sulfide doublet with a high QS. The value of QS strongly decreases with increasing sulfidation temperature. However, for CoNaY(dry) the resulting QS of 0.63 mm s^{-1} points to the presence of highly dispersed and/or disordered Co-sulfide species different from Co_9S_8.

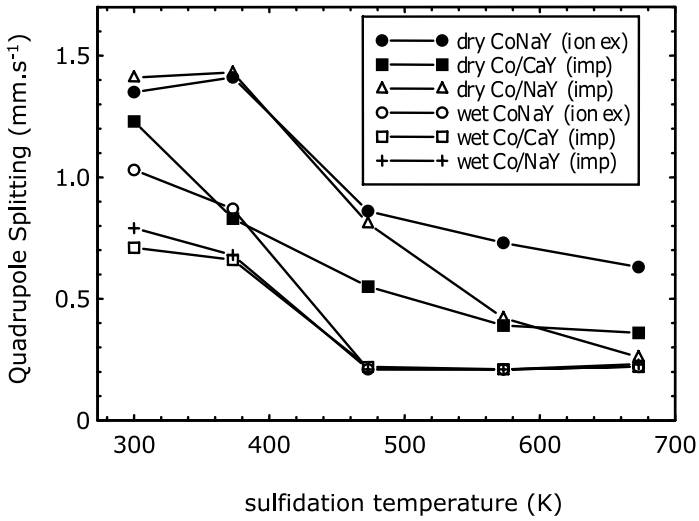

Fig. 5. The evolution of the quadrupole splitting of the doublets corresponding to 'Co-sulfide' and 'Co_9S_8' (QS = 0.19–0.27 mm s^{-1}) as a function of the sulfidation temperature. Wet sulfidation clearly results in bulky Co_9S_8-type phases, whereas dry sulfidation leads to dispersed/disordered Co-sulfide species. Moreover, these species are more disordered/smaller in the case of ion-exchange.

point to a mechanism where at elevated temperatures the Co-sulfide species react with the protons (initially generated upon Co^{2+} sulfidation) to form hydrogen sulfide and Co^{2+}. This protolysis reaction is in principle the reverse of reaction (4), albeit that the location of the Co cations is different. The resulting species are unique in the sense that they are not accessible to thiophene and cannot be resulfided. Such a protolysis reaction has been described before for NaY-supported Pt^0 and Ni^0 [84,85] and even at room temperature for CdS [86]. Vissenberg et al. [67] further pointed out that the protolysis reaction is retarded in sulfided CoCaY due to the preferential location of Ca^{2+} in the sodalite cages. Extensive work on NiNaY [18,40,64,69–71]

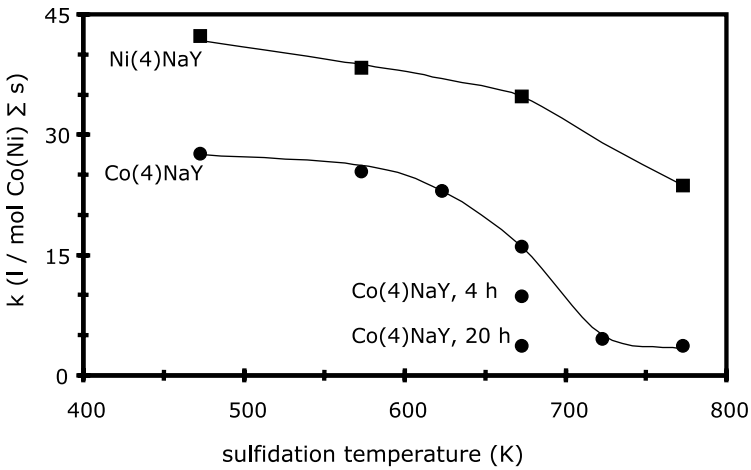

Fig. 6. The first-order reaction rate constant for thiophene hydrodesulfurization for CoNaY and NiNaY after various sulfidation treatments. Sulfidation was performed at the indicated temperatures for 2 h, except for two CoNaY samples that were sulfided for 4 and 20 h.

indicated that the nickel sulfide is well-dispersed in the micropores of NaY. While an ion-exchanged sample shows a quite high HDS activity, detailed elemental analysis suggests a predominance of Ni_3S_2 particles [71]. This result formed the basis for the quantum-chemical calculation of the full catalytic cycle of thiophene HDS over a Ni_3S_2 cluster by Neurock and van Santen [87]. Moreover, some indications were found that protolysis also occurs for sulfided NiNaY although more severe conditions (temperature above 773 K) are required [64]. Recently, Mariscal et al. [79] studied the stability of sulfided NiNaY in more detail. Protolysis of nickel sulfide species in He at 873 K was observed and confirmed by a blue shift of the infrared adsorption band of NO on sulfide species. Also in the case of NiHY, that proved more difficult to sulfide, a fraction of non-sulfidic Ni species was observed. From the NO IR study, it was concluded that nickel oxysulfide species formed by the protolysis reaction between nickel sulfide species and zeolite hydroxyl groups.

Potentially interesting is also the occlusion of Fe in the zeolite pores as a precursor to generate iron sulfide species which have some, but minor hydrogenation activity [88,89]. One of us (RvV) prepared Fe-containing USY and VUSY by refluxing the zeolitic materials in fairly concentrated $Fe(NO_3)_3$ solutions. The generation of a special dimer Fe site (Fig. 7) in (V)USY zeolite can be monitored by the reduction of the unit-cell size [90]. Its presence can be determined from IR spectra: Fig. 7 shows that the frequency of the TO_4 vibration depends on a_0 for dealuminated zeolites. Successful treatment with iron nitrate results in a lower vibration as expected. For a VUSY, the introduction of 2.5 wt.% Fe did not lead to the generation of such dimer sites and inspection of the IR bands in the hydroxyl region indicates ion-exchange. This is further corroborated by the Mössbauer spectrum in Fig. 7 showing the presence of some octahedral Fe^{3+} species. After sulfidation such materials perform similar to the starting VUSY. Treatment of USY (with $a_0 = 24.50$ Å), on the other hand, led to further dealumination, a_0 decreasing to 24.37 Å, and the formation of the special dimer site in line with IR observations. However, activity tests show that such material, when sulfided, perform similar to VUSY catalysts of the same unit-cell size. Specifically, the hydrogenation performance did not improve. Our conclusion is that $Fe(NO_3)_3$ treatment does not improve catalytic

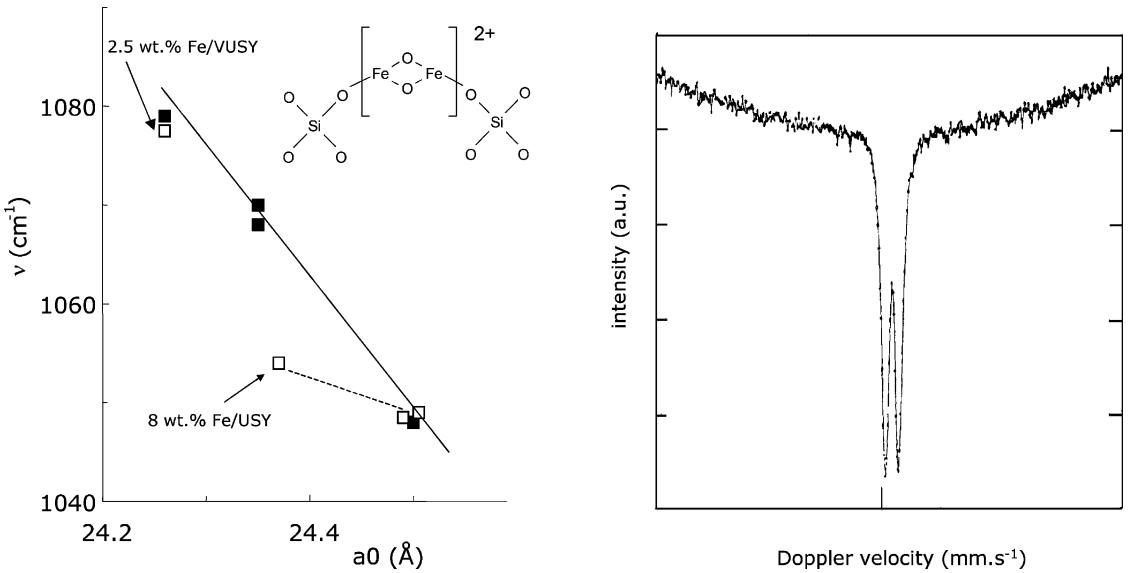

Fig. 7. Infrared frequencies of the framework TO_4 vibrations versus the unit-cell size for various supports (left: solid squares, (V)USY; open squares, after $Fe(NO_3)_3$ treatment; the solid line is taken from Ref. [88]) and room temperature ^{57}Fe Mössbauer spectrum of 2.5 wt.% Fe/VUSY prepared by refluxing the zeolite in a concentrated solution of $Fe(NO_3)_3$ (right). The inset shows the proposed dimer site coordinating to two aluminum-occupying tetrahedra.

performance beyond that of an unmodified material of the same unit-cell dimensions. Joyner et al. [91] recently reported on various methods to introduce FeS_x particles in ZSM-5 zeolite, interestingly noting that different Fe emplacement routes eventually led to similar FeS_x structures.

Although we limit the discussion largely to the incorporation of Co, Ni and Mo species in zeolite Y, we mention here the relative ease of incorporation of noble metals in dispersed form. For instance, Pt and Pd can be readily incorporated as amine complexes [e.g., 40,78,92-94]. Mostly, incompletely sulfided phases are formed, an important exception being the formation RuS_2-like particles in the zeolite pores. Work on intrazeolite Ru-sulfide species has resulted in an impressive body of work by the group of Breysse and co-workers [e.g., 95-98], that was recently extensively reviewed [7].

1.5. Organometallic complexes in well-defined zeolites

The difficulties encountered in the preparation of dispersed Mo and W species in the zeolite micropores have spurred research into the deposition of organometallic complexes in the micropore space which allow a better definition after adsorption in the micropore space. Zero-valent metal carbonyl complexes ($Mo(CO)_6$, $W(CO)_6$, $Ni(CO)_4$, $Co_2(CO)_8$, $Co(CO)_3NO$ and $Fe(CO)_5$) can be readily adsorbed in the supercages of zeolite NaY. The deposition of molybdenum hexacarbonyl has attracted the most attention [99–128]. Two $Mo(CO)_6$ molecules per supercage are adsorbed in NaY upon exposure to the vapor at room temperature [103,104,109,114]. Okamoto [122] showed that the loading strongly depends on the charge-compensating cation. Whereas Okamoto et al. [118] stressed the presence of six carbonyl species in the as-prepared precursor, de Bont et al. [123] found a loss of approximately one CO molecule by EXAFS. This was corroborated by the observation that these species can adsorb hydrogen sulfide at room temperature.

Thermal decarbonylation of encaged $Mo(CO)_6$ at low temperature [104,109,110] gives rise the formation of various subcarbonyl species, $Mo(CO)_x$ with $x = 3$–5. At low CO partial pressure, $Mo(CO)_3$ species are thermally most stable, but most reactive towards coordinating molecules [110,113,115] such as hydrogen sulfide [113]. Further heating in inert leads to clustering of Mo atoms [114], possibly partly present as metallic clusters on the external surface [112]. A further point to note is the relative high stability of the zeolite framework during incorporation of such carbonyl species, although several reports are not congruent [126,128]. Both thermal oxidation [118,119] or oxidation by UV-irradiation [118] results in small molybdenum(VI) oxide species in which the dimeric nature is preserved. Initial work involving sulfidation by Vrinat et al. [99] resulted in a poor dispersion to be attributed to the thermal decomposition of the hexacarbonyl species prior to sulfidation [113]. The group of Okamoto found that careful pretreatment and sulfidation of intrazeolite $Mo(CO)_6$ results in highly dispersed Mo-sulfide species, which are pronouncedly more active than catalysts prepared by AHM impregnation. Discrepancies between these results and those obtained by the group of de Beer [18,71] led to the conclusion that the presence of trace amounts of water during sulfidation is detrimental to the final dispersion [128]. This is exemplified by the TEM micrographs in Fig. 8 displaying the effect of the presence of water during sulfidation on the mobility of molybdenum sulfide species. In line with the results obtained earlier for CoNaY (vide supra), water molecules disturb the interaction with the zeolite framework inducing a higher mobility of metal sulfide species and their agglomeration on the external surface.

The highly dispersed nature of the species after sulfidation at 673 K was evidenced by NO adsorption [113,116] and Mo K-edge EXAFS measurements [119]. Essentially similar conclusions were obtained when the precursor was oxidized at relatively low temperature [119]. EXAFS measurements of stepwise sulfided encaged Mo clusters provides an effective method to analyze the evolution of the metal species [119,123]. Fig. 9 presents the stepwise sulfidation of zeolite-Y-encaged $Mo(CO)_6$. The presence of a Mo dimer in the precursor with a short Mo–Mo distance (2.80 Å) was noted (not shown). This dimer is partly preserved during sulfidation as evidenced by a Mo–Mo coordination number close to unity. Room temperature exposure to the sulfiding mixture leads to the adsorption of hydrogen sulfide. Mild sulfidation results in molybdenum dimer species with bridging

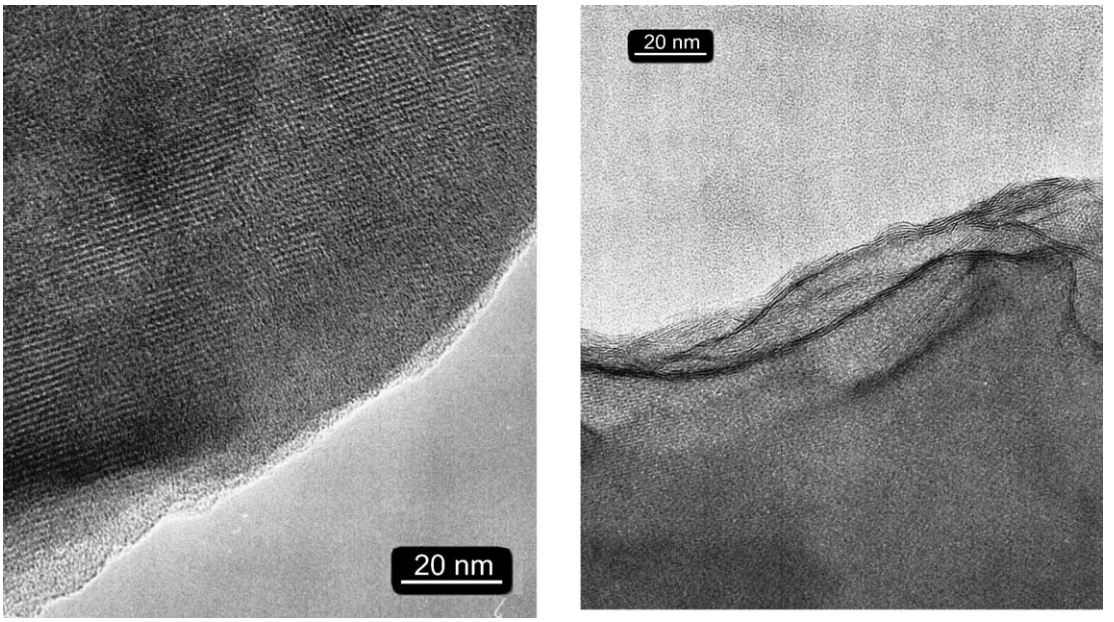

Fig. 8. TEM micrographs of $Mo(CO)_6$/NaY after dry sulfidation (left) and wet sulfidation (right). The presence of water in the H_2S/H_2 sulfiding mixture clearly results in the formation of MoS_2 slabs on the external zeolite surface.

S_2^{2-} and/or S^{2-} ligands. These species are thought to be MoS_3-like species which have been reported as intermediate species in the conversion of MoO_3 to MoS_2 [129,130]. Okamoto and Katsuyama [26] stressed that sulfidation at 673 K results in species with structural parameters close to those of crystalline MoS_2. This is in contrast to the results in Fig. 9 which indicate that a somewhat higher sulfidation temperature is necessary

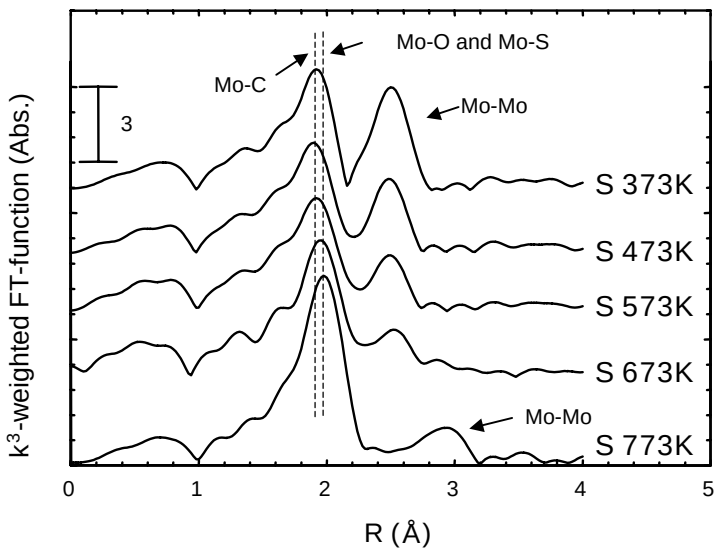

Fig. 9. k^3-Weighted Fourier transform functions (absolute part) of MoNaY sulfided at 373, 473, 573, 673 and 773 K. Clearly, the short Mo–Mo distance of around 2.8 Å is preserved after sulfidation at 673 K.

for the transformation to MoS_2-like species. This most probably derives from the stronger interaction between the Mo-sulfide complex and the zeolite lattice in our case compared to the zeolite used by the group of Okamoto, and is caused by differences in aluminum content of the zeolites [131]. Metal–metal coordination numbers close to unity are often taken as strong evidence for the prevailing presence of a binuclear cluster [119,123]. Okamoto and Katsuyama [119] rightfully raised doubts on such straightforward conclusions, since the EXAFS coordination numbers are also strongly affected by the disorder of the structure of the clusters. This initial suggestion [132] was further substantiated by Shido and Prins [133] for alumina-supported MoS_2. Nevertheless, the development of the coordination numbers in stepwise sulfidation experiments is a strong indication of the preservation of the highly dispersed nature of the resulting molybdenum sulfide species. Interestingly, Vissenberg [128] reported that very small Mo-sulfided particles sulfided at lower temperature with a characteristic Mo–Mo distance of 2.78 Å showed higher activity than those present after high-temperature sulfidation with a typical Mo–Mo distance of 3.16 Å.

The possibility to encage tungsten hexacarbonyl, $W(CO)_6$, has been employed less frequently [115,117,124,134–136]. Similar to $Mo(CO)_6$, two tungsten hexacarbonyl species can be deposited in the supercages. These species are somewhat more stable towards oxidation [124], but dimer W_2O_6 species have been found after oxidation [117] analogous to those in oxidized $Mo(CO)_6$/NaY.

The success in the use of well-defined zeolite-Y-encaged $Mo(CO)_6$ precursors to highly dispersed Mo-sulfide species has led to several investigations into the incorporation of cobalt carbonyl compounds [111,112,119,137]. The application of $Ni(CO)_4$ has been limited [138,139] for obvious toxicity reasons. Incorporation of the binuclear cobalt cluster, $Co_2(CO)_8$, in the zeolite Y pores results in its decomposition into $Co_4(CO)_{12}$ and Co subcarbonyl species [112] which are partly located on the external zeolite surface [111,112]. A more defined system is provided by incorporation of cobalt tricarbonylnitrosyl, $Co(CO)_3NO$ [67,111,119,137]. Thermal decomposition leads to the formation of metallic and oxidic Co species [111], while direct sulfidation results in the formation of dispersed cobalt sulfide species [67,117,137]. Recently, Kubota et al. [137] deposited this complex on several Y-type zeolites with a widely varying Si/Al ratio ranging from an almost silicious faujasite to NaY. Strikingly, the amount of adsorbed species relates to the amount of aluminum atoms in substitution positions of the zeolite matrix. The fact that all these zeolites were in their sodium form points to an interaction of the complex with these ions as described before for $Mo(CO)_6$ [112]. Concomitant with the increase in Co loading (with increasing Al content) the thiophene HDS activity of the sodium forms of the zeolites strongly decreased. Especially, sulfidation of $Co(CO)_3NO$ in the sodium form of USY ($Si/Al = 4.3$) results in almost atomically dispersed Co-sulfide particles with a very high intrinsic activity.

1.6. Mixed sulfides in zeolites

The genesis of highly active mixed Co(Ni)Mo(W) sulfides in the zeolite micropore space is attractive, since it may lead to the formation of a well-defined ‘Co–Mo–S’-type cluster. From preparative knowledge of alumina-supported catalysts, it is well known that the close proximity of the metals is a prerequisite for the formation of ‘Co–Mo–S’-type phases. This can be induced, for instance, by the presence of chelating agents such as nitrilo triacetic acid [140]. However, the size of such complexes is too large to pass through the zeolite entrances. Based on the earlier observation that the Anderson aluminomolybdate anion, $AlMo_6O_{24}H_6^{3-}$, could be accommodated in steamed zeolite Y [41] further work by the group of Payen [141] has been focussed on the incorporation of the ammonium salt of cobaltomolybdate, $(NH_4)_3(CoMo_6O_{24}H_6)$, in the secondary pores of zeolite Y with the advantage of a close proximity of Co and Mo in the precursor. A detailed characterization study revealed that the CoMo complex is preserved during impregnation. Calcination of the intact encaged cobaltomolybdate complex, however, results in its decomposition. Rehydration does not restore the CoMo complex, but rather the Anderson aluminomolybdate anion. As such, this method is not suitable to create a calcined CoMo precursor although it might be interesting to check the HDS activity of a sulfided, non-calcined precursor material. Recent attempts of our group to incorporate this cobaltomolybdate complex in the micropores of NaY were not successful

suggesting that the complexes in Payen's studies are indeed located in the secondary pore system.

Most preparation routes follow the impregnation of cobalt- or nickel-exchanged zeolite Y with AHM (or ammonium metatungstate, AMT) [28,30,142] and successive or co-impregnation of AHM (AMT) and Co- or Ni-nitrate [17,28,31,32,35,142,143]. The first method is preferred [28], because the Co precursor is more dispersed. Mostly, these catalysts display higher activities than their non-promoted counterparts providing an indication for the formation of some mixed sulfide phases. However, in the precursor Mo(W) and Ni(Co) are spatially separated making an efficient generation of promoted phases less likely. Further complicating factors are the difficulty in sulfiding the large MoO_3 aggregates on the external surface, leading to a low activity, the formation of α-$NiMoO_4$ [17] or α-$CoMoO_4$ phases, which also have a lower sulfidability and the beneficial influence of acidity generated upon sulfidation of cation-exchanged zeolites on the HDS activity. It is clear, however, that the presence of mesopores in ultrastabilized zeolites offers possibilities for the formation and better dispersion of MoS_2-type species and the possible presence of promoted MoS_2 phases [17,35].

Incorporation of molybdenum hexacarbonyl in well-dried Co-exchanged zeolite Y provides the necessary close proximity of the 'Co–Mo–S' metal constituents in the precursor material. This route was extensively studied by a combination of MES, EXAFS and TEM [144]. In line with the molybdenum-only case, two $Mo(CO)_6$ species can be incorporated in the supercages of dried Co^{2+}-exchanged NaY. In essence, ^{57}Co MES results indicate that the sulfidation of the Co^{2+} cations proceeds unperturbed by the presence of the Mo species. Finally, one ends up with highly dispersed Co-sulfide species which exhibit a strong interaction with the zeolite lattice. Analysis of EXAFS data indicates that also the sulfidation of the Mo dimer species is not hindered by the presence of Co, essentially giving similar dimer Mo-sulfide species as obtained after sulfidation of $Mo(CO)_6$/NaY. TEM micrographs stress the intrazeolite location of all metal sulfide species.

The similarity in MES parameters for the Co-sulfide species in sulfided CoMo/NaY and CoNaY is consistent with the well-dispersed nature of the species. This might explain the absence of a strong effect of the presence of Mo on the QS of the Co-sulfide species in the bimetallic catalyst. A more direct probe to observe Co–Mo interaction is possible by EXAFS. However, a detailed analysis of Co K-edge and Mo K-edge spectra of sulfided CoMo/NaY did not provide evidence for such interactions. Moreover, analysis of thiophene hydrodesulfurization activity data [128] shows that the catalytic activity of sulfided CoMo/NaY equals the sum of the activities of sulfided CoNaY and $Mo(CO)_6$/NaY. A possible explanation relates to the protolysis reaction described for sulfided CoNaY. Fig. 10 shows the MES spectra of CoMo/NaY and the Co K-edge XANES region. Although in first instance the MES spectra were fitted using two doublets corresponding to a Co-sulfide state (QS = 1.2 mm s^{-1}, ca. 30–40%) and a high-spin 2+ state (QS = 1.9 mm s^{-1}, ca. 60–70%), addition of a third one with a QS = 1.8 mm s^{-1} and IS = 0.6 mm s^{-1} improves the fitting. This unknown Co-doublet closely resembles the one observed for the high-temperature sulfided CoNaY species observed by Vissenberg et al. [64]. This resemblance is further underpinned by the observation that a He treatment at 673 K results in an increase of the contribution of this doublet from 20 to 35% (Fig. 10). Moreover, the XANES region clearly shows that after He treatment part of Co is experiencing an increased interaction with zeolite oxygen atoms. However, the intensity increase is lower than for CoNaY [144] stressing the protolysis is less extensive in the CoMo/NaY case.

The group of Okamoto reported the successful preparation of intrazeolite CoMo-sulfide clusters with a thiocubane structure [119,122,145,146]. Instead of Co^{2+} ion-exchange, gas-phase deposition of $Co(CO)_3NO$ is used followed by a first sulfidation step to produce small CoS_x particles. Subsequently, $Mo(CO)_6$ is introduced followed by a second sulfidation. Similar results were obtained by the reverse loading procedure. In both cases, a loading of approximately two Mo and two Co atoms per supercage was found. Most interestingly, a synergy in thiophene hydrodesulfurization was observed for such prepared materials with an optimum Co/Mo ratio of unity independent of the loading procedure. However, we note that the synergy in thiophene hydrodesulfurization [145] is much smaller than observed for alumina-supported mixed metal sulfides. Another indication of a Co–Mo interaction is provided by FTIR

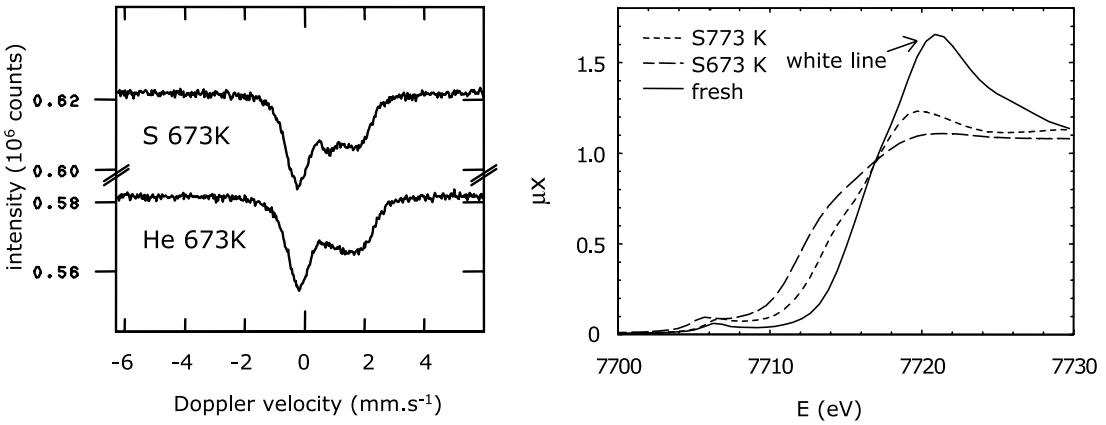

Fig. 10. MES spectra of CoMo/NaY sulfided at 673 K and treated in He at 673 K (left) and XANES region of the Co K-edge of CoMo/NaY of the fresh sample, the sample sulfided at 673 and 773 K (right). A third doublet corresponding to the unknown Co species generated upon protolysis of sulfided CoNaY is needed and grows upon helium treatment. This protolysis is also induced by high-temperature sulfidation as derived from the increase of the white line.

spectroscopy of adsorbed NO species [122]. Bands related to nitrosyl species on Co sites are identified, while those observed for sulfided $Mo(CO)_6$/NaY were removed. These observations suggest the relevance of Co sites in HDS catalysis. Although no quantitative EXAFS analysis of Co–Mo interactions is given, it is clear that a backscatterer is present at a distance of about 2.83 Å, close to that predicted from theory for Co–Mo distances [147]. A $Co_2Mo_2S_6$ cluster was proposed to be present in the zeolite pores [146]. The deviant conclusions of the work of de Bont et al. [144] on the one and Okamoto [145] on the other hand suggest that in CoS_x species deriving from sulfidation of Co^{2+} at cation-exchange positions are quite strongly bonded to the zeolite lattice, possibly an interaction with the generated acidic protons (vide infra). Moreover, differences in the interaction strength between the Mo species and the zeolite lattice may be important in explaining this discrepancy.

Taniguchi et al. [55] suggested the successful incorporation of $[Mo_3NiS_4Cl(H_2O)_9]^{3+}$, the bimetallic analogon of $[Mo_3S_4(H_2O)_9]^{4+}$ with a completed cubane structure, in zeolite Y. These authors found that NiMo/NaY were more active than Mo/NaY. The synergy was more pronounced in a catalyst derived from the bimetallic sulfide cluster than from a sample in which $[Mo_3S_4(H_2O)_9]^{4+}$ was ion-exchanged in a Ni^{2+}-exchanged zeolite. This again suggests that an intimate interaction between Ni and Mo in the precursor is important for the formation of highly active bimetallic phases.

1.7. Applications of models

Hydrodesulfurization of thiophenic compounds, e.g. thiophene, benzothiophene and dibenzothiophene, has been applied extensively to obtain insight into the catalytic properties of the sulfided precursors. Additional test reactions include hydrocracking and hydroisomerization. It is important to note here that also the acidic zeolite support itself exhibits an initially high activity in the desulfurization of thiophene [148]. The strong decrease observed for such metal-free zeolites is caused by extensive coke formation. The interaction of thiophene with acidic sites has been studied by quantum-chemical methods [149,150]. The deactivation is also observed for those metal-containing catalysts prepared from acidic zeolites or by sulfidation of transition metal ion-exchanged starting materials. The effect is enhanced by operation at atmospheric pressure where the imbalance between acidity and hydrogenation results in extensive coking [24,75]. This presents difficulties when comparing various catalysts: beneficial effects of acidic sites may be obscured when activity data are compared at prolonged reaction times and one should always check if a seemingly synergistic effect is larger than a simple additive one.

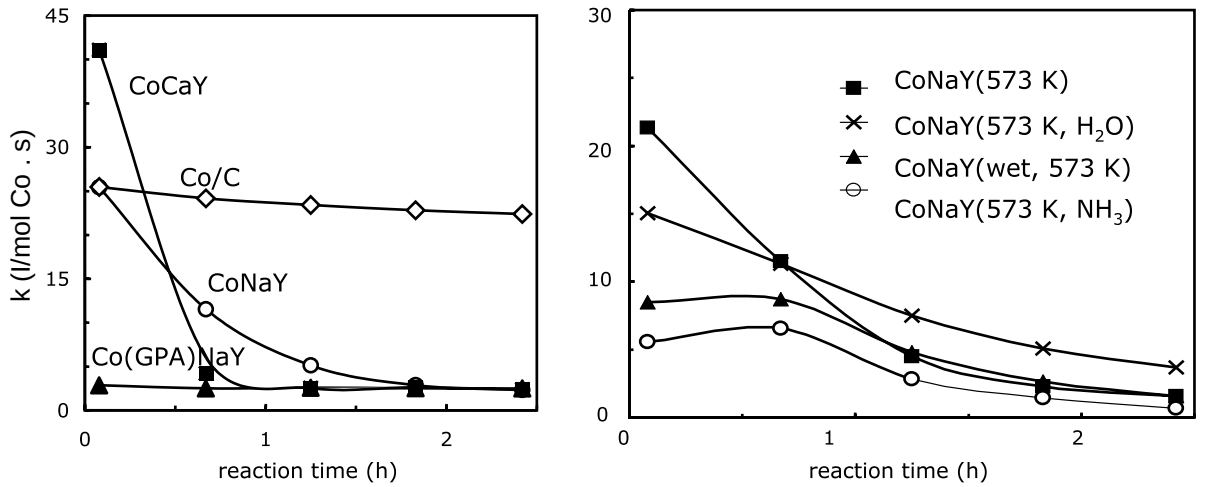

Fig. 11. Thiophene hydrodesulfurization activities of CoNaY(573 K), CoCaY(573 K), $Co(CO)_3NO$/NaY(573 K) and Co/C(673 K) (left) and CoNaY(573 K) after several treatments during (wet) and after (H_2O/NH_3) sulfidation (right) as a function of reaction time. The temperatures between brackets indicate the final sulfidation temperature.

This brings us to the questions we set out to answer in this report: what is the effect of the acidity on the intrinsic activity of zeolite-occluded metal sulfides and are there any special properties of very small metal sulfide particles? Fig. 11 displays the thiophene hydrodesulfurization activities for a series of zeolite-supported and a carbon-supported Co catalyst. The higher activity of the CoCaY compared to CoNaY is explained by the fact that the protolysis reaction is partly hindered due to the presence of Ca^{2+} in the sodalite cages [67]. The higher stability of the sample prepared by $Co(CO)_3NO$ deposition in the zeolite pores is caused by the absence of protons. Moreover, TEM results show that Co-sulfide particles from the $Co(CO)_3NO$ precursor have migrated to the external surface—in contrast to conclusions reached by Okamoto et al. [119,137]. As outlined before, the protolysis reaction for the sulfided cation-exchanged samples and the observation that the sulfide particles remain in the zeolite pores when carefully sulfided suggest an interaction between the metal sulfides and the zeolite protons. This was observed earlier for Pd metallic particles in zeolite Y [151]. Evidence for such an interaction is provided by treatment of the carefully sulfided catalysts with a base (water or ammonia), which results in a dramatic decrease of the activity (Fig. 11). The effects are similar to those obtained for wet sulfidation leading to the migration of Co-sulfide particles to the external zeolite surface [62,71] and is explained by the breaking of the interaction between the proton and the metal sulfide. Similar effects are noted for NiNaY [128]. It follows that for the preparation of well-defined, small Co-sulfide particles a strong interaction with the zeolite lattice is important. If absent—either due to the absence of protons (for $Co(CO)_3NO$ in NaY) or due to preferential adsorption of water on the protons during wet sulfidation [66,67]—metal sulfide aggregation occurs. Careful sulfidation of Co-exchanged faujasite, however, does result in anchoring of such species with a high initial activity. This bond can be broken relatively easily by a strong base. This poses a strong limitation for industrial use of these materials, because the nitrogen compounds and water present in crude oil will induce sintering of Co- or Ni-sulfide species.

A comparison of the intrinsic HDS activities of $Co(CO)_3NO$ in NaY, CaY and CoCaY [67] indicates that, in addition to the effect of dispersion, there is a positive effect of the acidity on the performance in line with earlier reports [75,148]. The exact nature of the synergistic effect is more difficult to ascertain. As forwarded by Welters et al. [148] the acidic sites may act as strong adsorption sites increasing the local concentration of thiophene close to the metal sulfide.

Alternatively, the acidity of the zeolite could further tune the catalytic properties of the metal sulfide through a direct interaction between the metal sulfide and the acidic proton or through modification of the strength of the bonding between metal-sulfide and zeolite framework. This latter notion is in line with the influence of protons on Ru-sulfide species [97] and with the recently reported synergism between CoMo-sulfide and an acidic ASA support [11,13,152]. An electronic influence of protons on the sulfide phase is also stressed in the work of Maugé by following the shift of the IR frequency of adsorbed CO [153].

A comparison of the activities of various cobalt-containing catalysts allows to conclude on the activity of very small metal sulfide particles. The initial activity of sulfided CoNaY is similar to that of sulfided Co/C. The former sample has a much higher dispersion (from EXAFS [65]) than sulfided Co/C (from MES [154,155]). Thus, the intrinsic activity of the Co-sulfide particles in Co/C is higher than that of ultra-dispersed particles in sulfided CoNaY. Hydrogen–deuterium equilibration results [156] over various Co-containing catalysts (Table 1) indicate that there is a clear relation between the equilibration activity and the quadrupole splitting of the sulfide phase. This is consistent with a higher activity for more dispersed Co-sulfide particles. This result and the structure-insensitive nature of the equilibration reaction further stress that the Co-sulfide dispersion in sulfided CoNaY is higher than in Co/C sulfided at 673 K. We thus infer that there must be an optimum cluster size for a high HDS activity. This positively answers the question if there are any special properties of very small particles albeit that the consequence for catalysis is a negative one. Additionally, one observes that the equilibration activity of a CoMo/C catalyst is one order of magnitude higher than that of an ultra-dispersed Co/C obtained after sulfidation at 373 K (and of Mo/C), both Co-containing catalysts exhibiting similar ^{57}Co Mössbauer parameters [81]. This resulted in the notion that besides the high dispersion of Co-sulfide particles on the edges of MoS_2 the creation of a new type of 'Co–Mo–S' site is responsible for the high activity of CoMo-based HDS catalysts [156]. Importantly, we observe that a sulfided CoMo/NaY sample with a highly dispersed Co-sulfide phase exhibits a relatively low equilibration activity compared to CoMo/C, further pointing to the absence of a Co–Mo interaction in these samples. In the zeolite case, sulfidation at 573 K does not produce MoS_2-type species. An additional equilibration experiment of a CoMo/NaY catalyst sulfided at 773 K showed a similar performance to a MoNaY catalyst sulfided at 773 K.

Table 1
Hydrogen–deuterium equilibration activities of a set of Co-containing carbon- and zeolite-supported catalysts and the quadrupole splitting (QS) of the Co-sulfide doublet

Catalyst	Rate (mol/mol h)[a]	QS (mm s^{-1})
Co/C (373 K)	0.15	1.08
Co/C (673 K)	0.02	0.39
Mo/C (673 K)	2.80	–
CoMo/C (673 K)	30.3	1.1
CoNaY (573 K)	0.11	0.73
MoNaY (773 K)	1.16	–
CoMoNaY (573 K)	0.66	1.15
CoMoNaY (773 K)	1.31	n.d.[b]

[a] Rates expressed per mole of Co except for Mo/C and Mo/NaY per mole of Mo.
[b] Not determined.

From the many detailed studies on sulfided $Mo(CO)_6$/NaY we can derive conclusions similar to the Co case. Fig. 12 compares the HDS activities of MoS_x species in $Mo(CO)_6$/NaY sulfided at various temperatures to those of titania- or alumina-supported MoS_2 species. The HDS activity of the zeolite-supported catalysts decreases with increasing sulfidation temperature. The decrease is most pronounced when the MoS_x species with a relatively short Mo–Mo coordination distance (~2.8 Å) are transformed in MoS_2-like species. Strikingly, a sample sulfided at 773 K—with Mo–S and Mo–Mo coordination distances close to those in MoS_2, but ultra-dispersed—exhibits a lower activity than MoS_2 species supported on alumina and titania with considerably lower MoS_2 dispersion. Analogous to the Co-sulfide case, this strongly suggests that there exists an optimum size of the MoS_2 clusters. Nevertheless, we observed that post-sulfidation treatment with bases does not decrease the catalytic activity of sulfided $Mo(CO)_6$/NaY, whereas wet sulfidation induces strong sintering [128]. Moreover, the low HDS activity for a sample prepared by sulfidation of $Mo(CO)_6$/HY [128] and its low dispersion (TEM) indicates that the interaction of MoS_x species with the basic framework oxygen atoms is more important

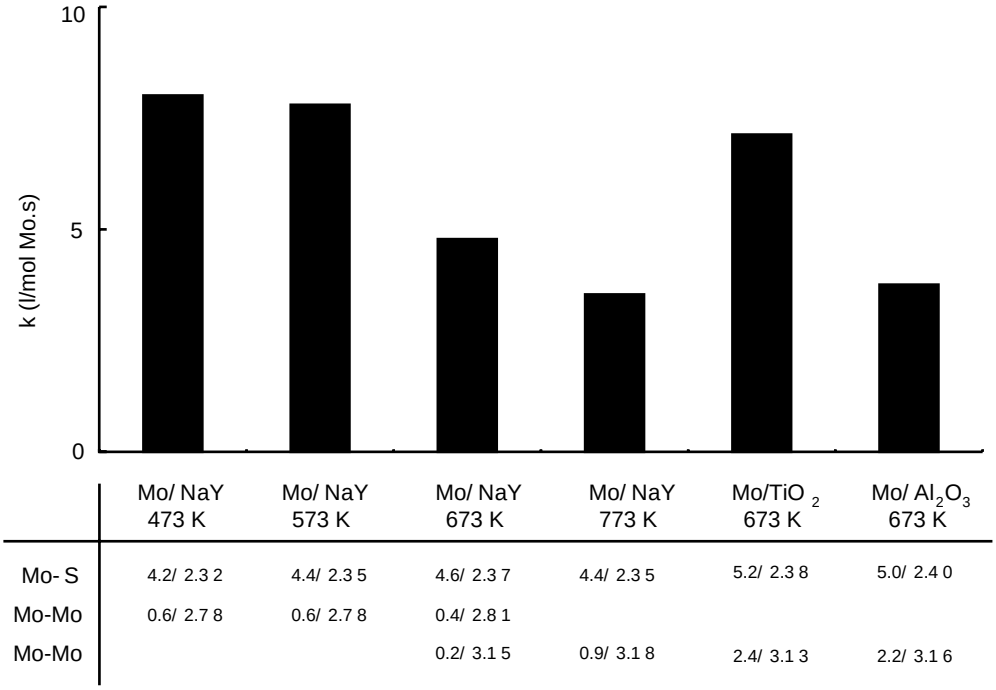

Fig. 12. Initial thiophene hydrodesulfurization activities of a suite of Mo-containing catalysts: Mo/NaY catalysts prepared by sulfidation at the indicated temperature of a $Mo(CO)_6$/NaY precursor, Mo/TiO_2 and Mo/Al_2O_3 prepared by pore-volume impregnation. The values below are fit parameters for multiple-shell data analysis of the Mo K-edge EXAFS of the sulfided samples (taken from Ref. [124]): indicated are the scatterer, the coordination number and coordination distance (in Å).

than the interaction with acidic protons. This result is in line with the difficulty in sulfiding low amounts of Mo on an alumina support [157] due to its strong interaction to the basic hydroxyl groups. Interestingly, the intrinsic activity of such a sample was shown to be higher than that of a fully sulfided sample.

The relatively low activities of these encaged monometallic sulfides cohere well with the absence of or the at most very minor synergism between Co and Mo occluded in the micropores. In that sense, we surmise that the more pronounced synergism observed in the $[Mo_3NiS_4Cl(H_2O)_9]^{3+}$-derived catalysts is related to the formation of 'Ni–Mo–S'-type species—induced by the intimate interaction of the two metals in the precursor—on the external surface rather than a high dispersion of an encaged NiMo-sulfide cluster. A NiMo/NaY catalyst had a slightly better performance than $NiMo/Al_2O_3$ [101].

Finally, an application test at Shell Research and Technolcogy Centre Amsterdam on commercial $NiW/VUSY\text{-}Al_2O_3$ onto which $Mo(CO)_6$ was deposited did not show any improvement against the Mo-free catalyst. Post-reaction TEM analysis clearly showed that the Mo-sulfide had been redistributed evenly throughout the catalyst sample. This is most probably caused by the presence of water during sulfidation and stresses the difficulties in keeping metal sulfides dispersed as small particles in the zeolite pores under industrial conditions. From an application point of view, the difficulty in keeping the hydrogenation function close to the acidic one is problematic. This makes it extremely difficult to study the 'proximity effect' for hydrocracking in detail. Nevertheless, some evidence, based in model NiNaY and NiMo/Y model systems [158–160], that the amount of coke formed is reduced with increased intimacy of mixing of the functions on the submicron level is available.

2. Conclusions

A suite of methods for the preparation of intrazeolite Co, Ni, Mo and W sulfides is reviewed. Conventional impregnation of Mo and W anions results in the external location of the metal oxide precursors, a poor dispersion of the resulting sulfide, incomplete sulfidation and partial amorphization of the zeolite lattice. In stabilized zeolites, part of the sulfide phase ends up in the mesopores. The use of cationic Mo species such as MoO_2^{2+} partly alleviates this problem, especially in the case of stabilized faujasite that is more resistant against acid attack. Sulfidation of carefully dried Co- or Ni-exchanged faujasite yields a well-dispersed metal sulfide phase concomitant with acidic protons. There is a clear synergistic effect on the thiophene HDS activity of such materials. The strong interaction between the sulfide and the acidic protons hinders agglomeration of the metal sulfide particles. Two problems related to possible applications are: (i) the loss of dispersion upon exposure to a base which displaces the metal sulfide from the proton and (ii) a protolysis reaction, mainly for Co-sulfide, resulting in a loss of catalytically active Co. The deposition of organometallic precursors such as $Mo(CO)_6$ also provides a route to well-dispersed metal sulfides upon sulfidation. The very dispersed nature of the initial dimeric Mo species in close interaction with the zeolite is retained up to quite high sulfidation temperatures. The transition from a dimeric species with a short Mo–Mo coordination distance and a high HDS activity to a species with structural parameters close to MoS_2 strongly decreases the activity. Attempts to prepare CoMo-sulfide clusters in the micropores of faujasite have not been too successful, although there are some indications that a CoMo-sulfide cluster is formed upon sulfidation of a sample prepared by introduction of both metals via their carbonyl clusters. However, the catalytic synergism is quite small.

Although the zeolite micropore space of faujasite forms a well-defined environment and in some cases allows the formation of occluded transition metal sulfide clusters, the exact structure of those species remains unclear. A pertinent conclusion, however, is that these very dispersed species exhibit lower HDS activities than larger ones supported on carbon, alumina or titania. Tentatively, this indicates that there is an optimum particle size for metal sulfides. Although the retention of metal sulfide particles in the zeolite cages is difficult—especially under industrial conditions—there is a beneficial effect of the close proximity of hydrogenation and acidic functions on the coking deactivation.

References

[1] I.V. Babich, J.A. Moulijn, Fuel 82 (2003) 607.
[2] P.J. Kooyman, E.J.M. Hensen, A.M. de Jong, J.W. Niemantsverdriet, J.A.R. van Veen, Catal. Lett. 74 (2001) 49.
[3] R. Prins, V.H.J. de Beer, G.A. Somorjai, Catal. Rev.-Sci. Eng. 31 (1989) 1.
[4] H. Topsøe, B.S. Clausen, F.E. Massoth, Hydrotreating Catalysis, Springer, Berlin, 1996.
[5] P.T. Vasudevan, J.L.G. Fierro, Catal. Rev.-Sci. Eng. 38 (1996) 161.
[6] S. Eijsbouts, Appl. Catal. A 158 (1997) 53.
[7] M. Breysse, E. Furimsky, S. Kasztelan, M. Lacroix, G. Perot, Catal. Rev. 44 (2002) 651.
[8] J. Scherzer, A.J. Gruia, Hydrocracking Science and Technology, Marcel Dekker, New York, 1996.
[9] I.E. Maxwell, J.K. Minderhoud, W.H.J. Stork, J.A.R. van Veen, in: G. Ertl, H. Knözinger, J. Weitkamp (Eds.), Handbook of Heterogeneous Catalysis, Wiley/VCH, New York/Weinheim, 1997, p. 2017.
[10] J.A.R. van Veen, in: M. Guisnet, J.-P. Gilson (Eds.), Zeolites for Cleaner Technologies, Imperial College Press, London, 2002, p. 131.
[11] E.J.M. Hensen, P.J. Kooyman, A.M. van der Kraan, Y. van der Meer, V.H.J. de Beer, J.A.R. van Veen, R.A. van Santen, J. Catal. 199 (2001) 224.
[12] M.J. Vissenberg, Y. van der Meer, E.J.M. Hensen, V.H.J. de Beer, A.M. van der Kraan, R.A. van Santen, J.A.R. van Veen, J. Catal. 198 (2001) 151–163.
[13] E.J.M. Hensen, V.H.J. de Beer, J.A.R. van Veen, R.A. van Santen, J. Catal. 215 (2003) 353.
[14] F. Schüth, Stud. Surf. Sci. Catal. 135 (2001) 1.
[15] J.A. Martens, E. Benazzi, J. Brendle, S. Lacombe, R. Led Dred, Stud. Surf. Sci. Catal. 130 (2000) 293.
[16] W.J.J. Welters, G. Vorbeck, H.W. Zandbergen, L.J.M. van de Ven, E.M. van Oers, J.W. de Haan, V.H.J. de Beer, R.A. van Santen, J. Catal. 161 (1996) 819.
[17] D. Li, H. Xu, G.D. Guthrie, J. Catal. 189 (2000) 281.
[18] G. Vorbeck, W.J.J. Welters, L.J.M. van de Ven, H.W. Zandbergen, J.W. de Haan, V.H.J. de Beer, R.A. van Santen, Stud. Surf. Sci. Catal. 84 (1994) 1617.
[19] M. Laniecki, W. Zmierczak Zeolites 11 (1991) 18.
[20] M. Laniecki, H.G. Karge, Stud. Surf. Sci. Catal. 94 (1995) 211.
[21] R. Cid, F.J. Gil Llabias, J.L.G. Fierro, A. Lopez Agudo, J. Villasenor, J. Catal. 89 (1984) 478.
[22] J.L.G. Fierro, J.C. Conesa, A. Lopez Agudo, J. Catal. 108 (1987) 334.

[23] J.L.G. Fierro, J.M. Rojo, J. Sanz, Colloids Surf. 15 (1985) 75.
[24] A. Lopez Agudo, R. Cid, F. Orellana, J.L.G. Fierro, Polyhedron 5 (1986) 187.
[25] J.A. Anderson, B. Pawelec, J.L.G. Fierro, Appl. Catal. A 99 (1993) 37.
[26] Y. Okamoto, H. Katsuyama, Ind. Eng. Chem. Res. 35 (1996) 1834.
[27] J. Thoret, C. Marchal, C. Doremieux-Morin, P.P. Man, M. Gruia, J. Fraissard, Zeolites 13 (1993) 269.
[28] R. Cid, F. Orellana, A. Lopez Agudo, Appl. Catal. 32 (1987) 327.
[29] C.P. Li, D.M. Hercules, J. Phys. Chem. 88 (1984) 456.
[30] V. Fornes, M. Vazquez, A. Corma, Zeolites 6 (1986) 125.
[31] J. Leglise, A. Janin, J.C. Lavalley, D. Cornet, J. Catal. 114 (1988) 388.
[32] A. Corma, M.I. Vazquez, A. Bianconi, A. Clozza, J. Garcia, O. Pallota, J.M. Cruz, Zeolites 8 (1988) 464.
[33] A. Ezzamarty, E. Catherine, D. Cornet, J.F. Hemidy, A. Janin, J.C. Lavalley, J. Leglise, in: P.A. Jacobs, R.A. van Santen (Eds.), Zeolites: Facts, Figures and Future, Elsevier, Amsterdam, 1989, p. 1025.
[34] J.A. Anderson, B. Pawelec, J.L.G. Fierro, P.L. Arias, F. Duque, J.F. Cambra, Appl. Catal. A 99 (1993) 55.
[35] J. Leglise, J.M. Manoli, C. Potvin, G. Djega-Mariadassou, D. Cornet, J. Catal. 152 (1995) 275.
[36] D. Cornet, M. El Qotbi, J. Leglise, Stud. Surf. Sci. Catal. 106 (1997) 147.
[37] B. Egia, J.F. Cambra, P.L. Arias, M.B. Guemez, J.A. Legarreta, B. Pawelec, J.L.G. Fierro, Appl. Catal. A 169 (1998) 37.
[38] E.J. Lede, F.G. Requejo, B. Pawelec, J.L.G. Fierro, J. Phys. Chem. B 106 (2002) 7823.
[39] J. Leglise, D. Cornet, M. Baalala, C. Potvin, J.-M. Manoli, Stud. Surf. Sci. Catal. 135 (2001) 4303.
[40] W.J.J. Welters, O.H. van der Waerden, H.W. Zandbergen, V.H.J. de Beer, R.A. van Santen, Ind. Eng. Chem. Res. 34 (1995) 1156.
[41] G. Plazenet, E. Payen, J. Lynch, B. Rebours, J. Phys. Chem. B 106 (2002) 7013.
[42] G.J. Hutchings, G. Buckles, Stud. Surf. Sci. Catal. B 49 (1989) 1413.
[43] R. Cid, J. Neira, J. Godoy, J.M. Palacios, S. Mendioroz, A. Lopez Agudo, J. Catal. 141 (1993) 206.
[44] K.S. Rawat, M.S. Rana, G. Murali Dhar, Stud. Surf. Sci. Catal. 135 (2001) 4248.
[45] E.L. Moorehead, US Patents 4 297 243 (1981), 4 388 224 (1983), 4 496 784 (1985).
[46] H. Minming, R.F. Howe, J. Catal. 108 (1987) 283.
[47] P. Dai, J.H. Lunsford, J. Catal. 64 (1980) 173.
[48] R.F. Howe, M. Jiang, S. Wong, J.H. Zhu, Catal. Today 6 (1989) 113.
[49] A.V. Kucherov, T.N. Kucherova, A.A. Slinkin, Kinet. Catal. 39 (1998) 732.
[50] M. Taniguchi, Y. Ishii, T. Murata, T. Tatsumi, M. Hidai, J. Chem. Soc., Chem. Commun. (1995) 2533.
[51] M. Taniguchi, S. Yasuda, Y. Ishii, T. Murata, M. Hidai, T. Tatsumi, Stud. Surf. Sci. Catal. 101 (1996) 107.
[52] T. Tatsumi, M. Taniguchi, S. Yasuda, Y. Ishii, T. Murata, M. Hidai, Appl. Catal. A 139 (1996) L5.
[53] T. Tatsumi, M. Taniguchi, H. Ishige, Y. Ishii, T. Murata, M. Hidai, Appl. Surf. Sci 121/122 (1997) 500.
[54] M. Jiang, T. Tatsumi, J. Phys. Chem. B 102 (1998) 10879.
[55] M. Taniguchi, D. Imamura, H. Ishige, Y. Ishii, T. Murata, M. Hidai, T. Tatsumi, J. Catal. 187 (1999) 139.
[56] M.R. Rigutto, J. Werner, Unpublished results.
[57] B. Sulikowski, J. Haber, A. Kubacka, K. Pamin, Z. Olejniczak, J. Ptaszynski, Catal. Lett. 39 (1996) 27.
[58] S.R. Mukai, T. Masuda, I. Ogino, K. Hashimoto, Appl. Catal. A 165 (1997) 219.
[59] Z. Olejniczak, B. Sulikowski, A. Kubacka, M. Gasior, Top. Catal. 11/12 (2000) 391.
[60] J.H. Lunsford, Rev. Inorg. Chem. 9 (1987) 1.
[61] T.I. Koranyi, A. Jentys, H. Vinek, Stud. Surf. Sci. Catal. 94 (1995) 582.
[62] P.W. de Bont, M.J. Vissenberg, E. Boellaard, R.A. van Santen, V.H.J. de Beer, A.M. van der Kraan, Bull. Soc. Chim. Belg. 104 (1995) 205.
[63] P.W. de Bont, M.J. Vissenberg, E. Boellaard, R.A. van Santen, V.H.J. de Beer, A.M. van der Kraan, in: I. Ortalli (Ed.), Proceedings of the Conference ICAME-95, vol. 50, Italian Physical Society, Bologna, 1995, p. 649.
[64] M.J. Vissenberg, P.W. de Bont, E.M. van Oers, R.A. de Haan, E. Boellaard, A.M. van der Kraan, V.H.J. de Beer, R.A. van Santen, Catal. Lett. 40 (1996) 25.
[65] P.W. de Bont, M.J. Vissenberg, E.L. Boellaard, V.H.J. de Beer, J.A.R. van Veen, R.A. van Santen, A.M. van der Kraan, J. Phys. Chem. B 101 (1997) 3072.
[66] M.J. Vissenberg, P.W. de Bont, J.W.C. Arnouts, L.J.M. van de Ven, J.W. de Haan, A.M. van der Kraan, V.H.J. de Beer, R.A. van Santen, Catal. Lett. 47 (1997) 155.
[67] M.J. Vissenberg, P.W. de Bont, W. Gruijters, V.H.J. de Beer, A.M. van der Kraan, R.A. van Santen, J.A.R. van Veen, J. Catal. 189 (2000) 209.
[68] R. Cid, J.L.G. Fierro, A. Lopez Agudo, Zeolites 10 (1990) 95.
[69] T.I. Koranyi, L.J.M. van de Ven, W.J.J. Welters, J.W. de Haan, V.H.J. de Beer, R.A. van Santen, Catal. Lett. 17 (1993) 105.
[70] T.I. Koranyi, L.J.M. van de Ven, W.J.J. Welters, J.W. de Haan, V.H.J. de Beer, R.A. van Santen, Colloid Surf. A 72 (1993) 143.
[71] W.J.J. Welters, G. Vorbeck, H.W. Zandbergen, V.H.J. de Beer, R.A. van Santen, J. Catal. 150 (1994) 155.
[72] R. Cid, J. Neira, J. Godoy, J.M. Palacios, A. Lopez Agudo, Appl. Catal. A 125 (1995) 169.
[73] T. Koranyi, F. Moreau, V. Rozanov, E.A. Rozanova, J. Mol. Struct. 410–411 (1997) 103.
[74] P.W. de Bont, M.J. Vissenberg, E. Boellaard, V.H.J. de Beer, J.A.R. van Veen, R.A. van Santen, Hyperfine Interact. 111 (1997) 39.
[75] R. Cid, J. Godoy, J. Neira, A. Lopez Agudo, J. Chem. Tech. Biotechnol. 72 (1998) 33.
[76] G. Niu, Y. Huang, Z. Cao, H. Zhisong, Y. Huang, Q. Li, Appl. Surf. Sci. 141 (1999) 35.

[77] R. Cid, P. Atanasova, R. Cordero, P.J.M. Lopez, A. Lopez Agudo, J. Catal. 182 (1999) 328.
[78] R. Navarro, B. Pawelec, J.L.G. Fierro, P.T. Vasudevan, J.F. Cambra, M.B. Guemez, P.L. Arias, Fuel Process. Technol. 61 (1999) 73.
[79] R. Mariscal, R.M. Navarro, B. Pawelec, J.L.G. Fierro, Micropor. Mesopor. Mater. 34 (2000) 181.
[80] J.P.R. Vissers, V.H.J. de Beer, R. Prins, J. Chem. Soc., Faraday Trans. 1 (83) (1987) 2145.
[81] M.W.J. Crajé, Ph.D. Thesis, Interfacultair Reactor Instituut, Delft University of Technology, Delft, The Netherlands, 1992. ISBN 90-73861-08-X.
[82] T.I. Morrison, A.H. Reis, E. Gebert, L.E. Iton, G.D. Stucky, S.L. Suib, J. Chem. Phys. 72 (1980) 6276.
[83] P. Gallezot, B. Imelik, J. Chim. Phys. Phys.-Chim. Biol. 71 (1974) 155.
[84] M.S. Tzou, B.K. Teo, W.M.H. Sachtler, J. Catal. 113 (1988) 220.
[85] H.J. Jiang, M.S. Tzou, W.M.H. Sachtler, Catal. Lett. 1 (1988) 99.
[86] N. Herron, Y. Wang, M.M. Eddy, G.D. Stucky, D.E. Cox, K. Moller, T. Bein, J. Am. Chem. Soc. 111 (1989) 530.
[87] M. Neurock, R.A. van Santen, J. Am. Chem. Soc. 116 (1994) 4427.
[88] Y. Maeda, N. Kato, S. Kawasaki, Y. Takashima, S. Hidaka, K. Nita, Zeolites 10 (1990) 21.
[89] K. Inamura, R. Iwamoto, in: M. Absi-Halabi, et al. (Eds.), Catalysts in Petroleum Refining and Petrochemical Industries, 1995, Elsevier, Amsterdam, 1996, p. 543.
[90] S. Hideka, A. Iino, M. Gotoh, N. Ishikawa, T. Mibuchi, K. Nita, Appl. Catal. 43 (1988) 57.
[91] R.W. Joyner, M. Stockenhuber, O.P. Tkachenko, Catal. Lett. 85 (2003) 193.
[92] M. Sugioka, C. Tochiyama, F. Sado, N. Maesaki, Stud. Surf. Sci. Catal. 100 (1996) 551.
[93] H. Yasuda, N. Matsubayashi, T. Sato, Y. Yoshimura, Catal. Lett. 54 (1998) 23.
[94] H.R. Reinhoudt, R. Troost, A.D. van Langeveld, J.A.R. van Veen, S.T. Sie, J.A. Moulijn, Stud. Surf. Sci. Catal. 127 (1999) 251.
[95] S. Gobolos, M. Lacroix, T. Decamp, M. Vrinat, M. Breysse, Bull. Soc. Chim. Belg. 100 (1991) 907.
[96] B. Moraweck, G. Bergeret, M. Cattenot, V. Kougionas, C. Genatet, J.-L. Portefaix, J.L. Zotin, M. Breysse, J. Catal. 165 (1997) 45.
[97] M. Breysse, M. Cattenot, V. Kougionas, J.C. Lavalley, F. Mauge, J.L. Portefaix, J.L. Zotin, J. Catal. 168 (1997) 143.
[98] C. Dumonteil, M. Lacroix, C. Geantet, H. Jobic, M. Breysse, J. Catal. 187 (1999) 464.
[99] M. Vrinat, C. Gachet, L. De Mourgues, Stud. Surf. Sci. Catal. 5 (1980) 219.
[100] S. Namba, T. Komatsu, T. Yashima, Chem. Lett. 1 (1982) 115.
[101] S. Abdo, R.F. Howe, J. Phys. Chem. 87 (1983) 1722.
[102] M.B. Ward, K. Mizuno, J.H. Lunsford, J. Mol. Catal. 27 (1984) 1.
[103] T. Komatsu, S. Namba, T. Yashima, K. Domen, T. Onishi, J. Mol. Catal. 33 (1985) 345.
[104] Y.S. Yong, R.F. Howe, Stud. Surf. Sci. Catal. 28 (1986) 883.
[105] A. Maezawa, H. Kane, Y. Okamoto, T. Imanaka, Chem. Lett. (1987) 241.
[106] T. Komatsu, T. Yashima, J. Mol. Catal. 40 (1987) 83.
[107] A. Kazusaka, R.F. Howe, J. Catal. 111 (1988) 50.
[108] Y. Okamoto, H. Kane, T. Imanaka, Catal. Lett. 12 (1988) 2005.
[109] Y. Okamoto, A. Maezawa, H. Kane, I. Mitsushima, T. Imanaka, J. Chem. Soc., Faraday Trans. 1 (84) (1988) 851.
[110] Y. Okamoto, A. Maezawa, H. Kane, T. Imanaka, J. Catal. 112 (1988) 585.
[111] S.L.T. Anderson, R.F. Howe, J. Phys. Chem. 93 (1989) 4913.
[112] C. Bremard, E. Denneulin, C. Depecker, P. Legrand, Stud. Surf. Sci. Catal. 48 (1989) 219.
[113] Y. Okamoto, A. Maezawa, H. Kane, T. Imanaka, J. Mol. Catal. 52 (1989) 337.
[114] J.M. Coddington, R.F. Howe, Y.S. Yong, K. Asakura, Y. Iawasawa, J. Chem. Soc., Faraday Trans. 86 (1990) 1015.
[115] S. Ozkar, G.A. Ozin, K. Moller, T. Bein, J. Am. Chem. Soc. 112 (1990) 9575.
[116] M. Laniecki, W. Zmierczak, Stud. Surf. Sci. Catal. 69 (1991) 331.
[117] G.A. Ozin, R.A. Prokopowicz, S. Ozkar, J. Am. Chem. Soc. 114 (1992) 8953.
[118] Y. Okamoto, Y. Kobayashi, T. Imanaka, Catal. Lett. 20 (1993) 49.
[119] Y. Okamoto, H. Katsuyama, Stud. Surf. Sci. Catal. 101 (1996) 503.
[120] Y. Sakamoto, N. Togashi, O. Terasaki, T. Ohsuna, Y. Okamoto, K. Hiraga, Mater. Sci. Eng. A 217/218 (1996) 147.
[121] Y. Okamoto, H. Katsuyama, K. Yoshida, K. Nakai, M. Matsuo, Y. Sakomoto, J. Yu, O. Terasaki, J. Chem. Soc., Faraday Trans. 92 (1996) 4647.
[122] Y. Okamoto, Catal. Today 39 (1997) 45.
[123] P.W. de Bont, M.J. Vissenberg, V.H.J. de Beer, J.A.R. van Veen, R.A. van Santen, A.M. van der Kraan, Appl. Catal. A 202 (2000) 99.
[124] Y. Okamoto, T. Kubota, Micropor. Mesopor. Mater. 48 (2001) 301.
[125] T. Shido, A. Yamaguchi, Y. Inada, K. Asakura, M. Nomura, Y. Iwasawa, Top. Catal. 18 (2002) 53.
[126] Y. Okamoto, N. Oshima, Y. Kobayashi, O. Terasaki, T. Kodaira, T. Kubota, PCCP 4 (2002) 2852.
[127] A. Yamaguchi, A. Suzuki, T. Shido, Y. Inada, K. Asakura, M. Nomura, Y. Iwasama, J. Phys. Chem. B 106 (2002) 2415.
[128] M.J. Vissenberg, Ph.D. Thesis, Eindhoven University of Technology, Eindhoven, The Netherlands, 1999. ISBN 90-386-0940-X.
[129] S.P. Cramer, K.S. Liang, A.J. Jacobsen, C.H. Chang, R.R. Chianelli, Inorg. Chem. 23 (1984) 1215.
[130] T. Weber, J.C. Muijsers, J.W. Niemantsverdriet, J. Phys. Chem. 99 (1995) 9194.
[131] Y. Okamoto, Personal communication.
[132] R.R. Chianelli, M. Daage, M.J. Ledoux, Adv. Catal. 40 (1994) 177.
[133] T. Shido, R. Prins, J. Phys. Chem. B 102 (1998) 8426.

[134] K. Moller, T. Bein, S. Ozkar, G.A. Ozin, J. Phys. Chem. 95 (1991) 5276.
[135] C. Bremard, M. Le Maire, J. Mol. Struct. 349 (1995) 49.
[136] S.D. Djajanti, R.F. Howe, Stud. Surf. Sci. Catal. 97 (1995) 197.
[137] T. Kubota, H. Okamoto, Y. Okamoto, Catal. Lett. 67 (2000) 171.
[138] K. Rao, S. Mohana, A. Zecchina, Langmuir 5 (1989) 319.
[139] N. Kumar Indu, H. Hobert, I. Weber, J. Datka, Zeolites 15 (1995) 714.
[140] J.A.R. van Veen, E. Gerkema, A.M. van der Kraan, A. Knoester, J. Chem. Soc., Chem. Commun. (1987) 1684.
[141] G. Plazenet, E. Payen, J. Lynch, PCCP 4 (2002) 3924.
[142] S. Bendezu, R. Cid, J.L.G. Fierro, A. Lopez Agudo, Appl. Catal. A 197 (2001) 47.
[143] R. Cid, F.G. Gil Llabias, M. Gonzalez, A. Lopez Agudo, Catal. Lett. 24 (1994) 147.
[144] P.W. de Bont, M.J. Vissenberg, E.J.M. Hensen, V.H.J. de Beer, J.A.R. van Veen, R.A. van Santen, Appl. Catal. A 236 (2002) 205.
[145] Y. Okamoto, in: M. Absi-Halabi, et al. (Eds.), Catalysts in Petroleum Refining and Petrochemical Industries, 1995, Elsevier, Amsterdam, 1996, p. 77.
[146] Y. Okamoto, H. Okamoto, T. Kubota, H. Kobayashi, O. Terasaki, J. Phys. Chem. B 103 (1999) 7160.
[147] S.M.A.M. Bouwens, F.B.M. van Zon, M.P. van Dijk, A.M. van der Kraan, V.H.J. de Beer, J.A.R. van Veen, D.C. Koningsberger, J. Catal. 146 (1994) 375.
[148] W.J.J. Welters, V.H.J. de Beer, R.A. van Santen, Appl. Catal. A 119 (1994) 253.
[149] X. Rozanska, X. Saintigny, R.A. van Santen, S. Clémendot, F. Hutschka, J. Catal. 208 (2002) 89.
[150] X. Rozanska, R.A. van Santen, F. Hutschka, Stud. Surf. Sci. Catal. 135 (2001) 2611.
[151] Z. Zhang, B. Lerner, G.-D. Lei, W.M.H. Sachtler, J. Catal. 140 (1993) 481.
[152] W.R.A.M. Robinson, J.A.R. van Veen, V.H.J. de Beer, Fuel Process. Technol. 61 (1999) 89.
[153] G. Crépeau, Ph.D. Thesis, Université de Caen, Caen, France, 2002.
[154] M.W.J. Crajé, V.H.J. de Beer, A.M. van der Kraan, Appl. Catal. 70 (1991) L7.
[155] M.W.J. Crajé, V.H.J. de Beer, A.M. van der Kraan, Hyperfine Interact. 69 (1991) 795.
[156] E.J.M. Hensen, G.M.H.J. Lardinois, V.H.J. de Beer, J.A.R. van Veen, R.A. van Santen, J. Catal. 187 (1999) 95.
[157] E.J.M. Hensen, V.H.J. de Beer, J.A.R. van Veen, R.A. van Santen, Catal. Lett. 84 (2002) 59.
[158] W.J.J. Welters, Ph.D. Thesis, Eindhoven University of Technology, Eindhoven, The Netherlands, 1994.
[159] J.L. Lemberton, M. Touzeyido, M. Guisnet, Appl. Catal. 54 (1989) 101.
[160] J.L. Lemberton, M. Touzeyido, M. Guisnet, Appl. Catal. 54 (1989) 115.